

DESIGN OF ENERGY-EFFICIENT APPROXIMATE ARITHMETIC CIRCUITS

A Thesis

by

BOTANG SHAO

Submitted to the Office of Graduate and Professional Studies of
Texas A&M University
in partial fulfillment of the requirements for the degree of

MASTER OF SCIENCE

Chair of Committee,	Peng Li
Committee Members,	Seong Gwan Choi
	Rabi N. Mahapatra
Head of Department,	Chanan Singh

August 2014

Major Subject: Computer Engineering

Copyright 2014 Botang Shao

ABSTRACT

Energy consumption has become one of the most critical design challenges in integrated circuit design. Arithmetic computing circuits, in particular array-based arithmetic computing circuits such as adders, multipliers, squarers, have been widely used. In many cases, array-based arithmetic computing circuits consume a significant amount of energy in a chip design. Hence, reduction of energy consumption of array-based arithmetic computing circuits is an important design consideration. To this end, designing low-power arithmetic circuits by intelligently trading off processing precision for energy saving in error-resilient applications such as DSP, machine learning and neuromorphic circuits provides a promising solution to the energy dissipation challenge of such systems.

To solve the chip's energy problem, especially for those applications with inherent error resilience, array-based approximate arithmetic computing (AAAC) circuits that produce errors while having improved energy efficiency have been proposed. Specifically, a number of approximate adders, multipliers and squarers have been presented in the literature. However, the chief limitation of these designs is their un-optimized processing accuracy, which is largely due to the current lack of systemic guidance for array-based AAAC circuit design pertaining to optimal tradeoffs between error, energy and area overhead.

Therefore, in this research, our first contribution is to propose a general model for approximate array-based approximate arithmetic computing to guide the

minimization of processing error. As part of this model, the Error Compensation Unit (ECU) is identified as a key building block for a wide range of AAAC circuits. We develop theoretical analysis geared towards addressing two critical design problems of the ECU, namely, determination of optimal error compensation values and identification of the optimal error compensation scheme. We demonstrate how this general AAAC model can be leveraged to derive practical design insights that may lead to optimal tradeoffs between accuracy, energy dissipation and area overhead. To further minimize energy consumption, delay and area of AAAC circuits, we perform ECU logic simplification by introducing don't cares.

By applying the proposed model, we propose an approximate 16x16 fixed-width Booth multiplier that consumes 44.85% and 28.33% less energy and area compared with theoretically the most accurate fixed-width Booth multiplier when implemented using a 90nm CMOS standard cell library. Furthermore, it reduces average error, max error and mean square error by 11.11%, 28.11% and 25.00%, respectively, when compared with the best reported approximate Booth multiplier and outperforms the best reported approximate design significantly by 19.10% in terms of the energy-delay-mean square error product (EDE_{ms}).

Using the same approach, significant energy consumption, area and error reduction is achieved for a squarer unit, with more than 20.00% EDE_{ms} reduction over existing fixed-width squarer designs. To further reduce error and cost by utilizing extra signatures and don't cares, we demonstrate a 16-bit fixed-width squarer that improves the energy-delay-max error (EDE_{max}) by 15.81%.

DEDICATION

To my parents and twin brother

ACKNOWLEDGEMENTS

It would not have been possible for me to finish such a project that involves a large number of principles, experiments and various methods without the help and encouragement of many people.

First and most importantly, I would like to thank my advisor Prof. Peng Li, who supported me for the project and gave me so much guidance and help with great patience during the last fifteen months. Whenever I had problems on the project, he would give me suggestions by meetings or sending emails, even when it was late at night. Prof. Li had such a significant impact on me with his hard work, dedication to perfection and excellence and enthusiasm for research, which will also impact significantly on my future work in industry.

Secondly, many thanks to Prof. Mahapatra and Prof. Choi who spent time attending my defense and helped improve my research by giving me many valuable suggestions on the project.

I would also like to remember and thank for my lab partners, Qian Wang, Honghuang Lin, Jingwei Xu, Ahmad Bashaireh and Yongtae Kim who gave me suggestions and much help for the usage of tools and software.

Last but not least, I would like to express my sincere acknowledgement to my parents and twin brother. They kept encouraging me when I was in trouble and especially, I got much encouragement from my twin brother who is now a PhD student in one of the best medical universities in China and is working so hard on his research.

TABLE OF CONTENTS

	Page
ABSTRACT	ii
DEDICATION	iv
ACKNOWLEDGEMENTS	v
TABLE OF CONTENTS	vi
LIST OF FIGURES.....	viii
LIST OF TABLES	x
1. INTRODUCTION.....	1
1.1 Motivation	1
1.2 Previous work.....	3
1.2.1 Approximate multipliers.....	3
1.2.2 Approximate squarers.....	4
2. ARRAY-BASED APPROXIMATE ARITHMETIC COMPUTING (AAAC) MODEL.....	5
2.1 Error Metrics	6
2.2 Model of Error Compensation Unit (ECU).....	7
2.3 Ideal Error Compensation & ECU Design.....	9
2.4 Further Reduction of Error and Cost.....	13
2.5 Practical ECU Design Guidance	16
3. PROPOSED MULTIPLIER DESIGN	18
3.1 Fundamentals of Booth Multipliers.....	18
3.2 The Basic Idea.....	19
3.3 Design of Error Compensation Unit.....	24
3.4 The Complete Fixed-Width Multiplier	28
3.5 Proposed Full-Width Booth Multiplier	29
4. PROPOSED SQUARER DESIGN	31
4.1 The Basic Squarer Design	31
4.2 Further Error and Cost Reduction for Fixed-Width Squarers	33
5. COMPRESSORS FOR MULTIPLIER AND SQUARER DESIGN.....	36

5.1 2:2 Compressors	37
5.2 3:2 Compressors	38
5.3 4:2 (5:3) Compressors	39
5.4 Using Compressors to Compress Array-Based Partial Product Table	39
6. EXPERIMENTAL RESULTS	42
6.1 Comparison of Different Multipliers	43
6.2 Accuracy Analysis for the Approximate Multipliers	45
6.2.1 Fixed-Width Booth Multipliers	45
6.2.2 Full-Width Booth Multipliers	50
6.3 Comparison of Different Squarers	54
6.4 Accuracy Analysis for Squarers	56
6.4.1 Fixed-Width Squarers	56
6.4.2 Full-Width Squarers	60
6.5 Further Reduction of Error and Cost For the 16-bit Fixed-Width Squarer	63
7. CONCLUSION	66
REFERENCES	67

LIST OF FIGURES

	Page
Figure 1. Arithmetic computing unit models: (a) Error-Free Computing Unit (EFCU) model (large energy consumption, area and delay), (b) Proposed AAAC model (small energy consumption, area and delay).	5
Figure 2. ECU model: (a) Signature generator, (b) Fixed compensation per input group.	8
Figure 3. Classification of the inputs based on the signatures.	9
Figure 4. A 4-group example for Theorem 4.	12
Figure 5. Error-Free Booth multiplier blocks.....	18
Figure 6. Schematics of Radix-4 Booth encoding block: (a) Schematic of s_i, d_i generation, (b) Schematic of n_i generation, (c) Schematic of z_i generation, (d) Schematic of c_i generation.	20
Figure 7. Schematic of the selection block.	21
Figure 8. Partial product diagram for fixed-width 16x16 bits Booth multipliers (n=16).	21
Figure 9. Blocks and schematics of Signature Generator.	27
Figure 10. Blocks of sorting network.....	27
Figure 11. Squaring diagram for 16-bit fixed-width squarers.....	31
Figure 12. Complete designs blocks: (a) the proposed multipliers, (b) the proposed squarers.	37
Figure 13. Block diagram of a 2:2 compressor.	38
Figure 14. Blocks of a 3:2 compressor.....	38
Figure 15. Using 2:2 and 3:2 compressors to compress an array-based partial product table.....	40
Figure 16. EDE_{ms} reduction of the proposed 16x16 bits fixed-width multipliers over DTM, PTM, PEBM and ZSM.	44

Figure 17. Error reduction of the proposed 8x8 fixed-width Booth multiplier over DTM, PEBM, ZSM.	46
Figure 18. Error reduction of the proposed 12x12 fixed-width Booth multiplier over DTM, PEBM, ZSM.	47
Figure 19. Error reduction of the proposed 16x16 fixed-width Booth multiplier over DTM, PEBM, ZSM.	48
Figure 20. Error reduction of the proposed 32x32 fixed-width Booth multiplier over DTM, PEBM, ZSM.	49
Figure 21. Error reduction of the proposed 8x8 full-width Booth multiplier over PEBM, ZSM.	50
Figure 22. Error reduction of the proposed 12x12 full-width Booth multiplier over PEBM, ZSM.	51
Figure 23. Error reduction of the proposed 16x16 full-width Booth multiplier over PEBM, ZSM.	52
Figure 24. Error reduction of the proposed 32x32 full-width Booth multiplier over PEBM, ZSM.	53
Figure 25. EDE_{ms} reduction of the proposed 16-bit fixed-width squarer over DTS, PTS, CCS and VCS.	55
Figure 26. Error reduction of the proposed 8-bit fixed-width squarer over DTS, CCS, VCS.	57
Figure 27. Error reduction of the proposed 12-bit fixed-width squarer over DTS, CCS, VCS.	58
Figure 28. Error reduction of the proposed 16-bit fixed-width squarer over DTS, CCS, VCS.	59
Figure 29. Error reduction of the proposed 8-bit full-width squarer over CCS, VCS.	60
Figure 30. Error reduction of the proposed 12-bit full-width squarer over CCS, VCS. ...	61
Figure 31. Error reduction of the proposed 16-bit full-width squarer over CCS, VCS. ...	62
Figure 32. Comparison of EDE_{max} of 16-bit fixed-width squarers with extra input signatures.	64

LIST OF TABLES

	Page
Table 1. Signals of Radix-4 Booth encoding.	25
Table 2. Compensation for input groups of 16x16 multiplier.	29
Table 3. Optimal compensation for the refined input groups.	29
Table 4. Compensation for input cases of 16-bit squarer.	32
Table 5. Compensation for input groups of 16-bit squarer.	33
Table 6. Implementation results of different 16x16 bits fixed-width Booth multipliers.	43
Table 7. EDE_{ms} of 16x16 fixed-width multipliers.	44
Table 8. Error metrics of 8x8 fixed-width Booth multipliers.	45
Table 9. Error metrics of 12x12 fixed-width Booth multipliers.	46
Table 10. Error metrics of 16x16 fixed-width Booth multipliers.	47
Table 11. Error metrics of 8x8 full-width Booth multipliers.	50
Table 12. Error metrics of 12x12 full-width Booth multipliers.	51
Table 13. Error metrics of 16x16 full-width Booth multipliers.	52
Table 14. Implementation results of different 16x16 bits fixed-width squarers.	54
Table 15. EDE_{ms} of 16x16 bits fixed-width squarers.	55
Table 16. Error metrics of 8-bit fixed-width squarers.	56
Table 17. Error metrics of 12-bit fixed-width squarers.	58
Table 18. Error metrics of 16-bit fixed-width squarers.	59
Table 19. Error metrics of 8-bit full-width squarers.	60
Table 20. Error metrics of 12-bit full-width squarers.	61
Table 21. Error metrics of 16-bit full-width squarers.	62

Table 22. Optimal extra signatures for given number of extra signatures.	63
Table 23. EDE_{max} of 16-bit fixed-width squarers with extra signatures.....	64

1. INTRODUCTION

1.1 Motivation

As the CMOS technology and VLSI design complexity scale, delivering desired functionalities while managing chip power consumption has become a first-class design challenge. To remedy this grand energy-efficiency challenge, approximate arithmetic circuits, in particular array-based approximate arithmetic computing (AAAC) circuits, have been introduced as a promising solution to applications with inherent error resilience including media processing, machine learning and neuromorphic systems. AAAC may allow one to trade off accuracy for significant reduction of energy consumption for such error tolerant applications.

To this end, approximate multipliers and squarers have been a focus of a great deal of past and ongoing work. Two types of approximate multipliers exist: approximate AND-array multipliers, which utilize AND gates for partial product generation [1]-[2] and approximate Booth multipliers [3]-[8], which use the modified Booth algorithm to reduce the number of partial products. For squarer units, a series of approximate squarers have been proposed [9]-[11].

While a diverse set of array-based approximate arithmetic unit designs exist, what is currently lacking is systemic design guidance that allows one to optimally tradeoff between error, area and energy. While the area and energy of a given design can often be easily reasoned or estimated, getting insights on error and thereby providing a

basis for optimally trading off between error, area and energy consumption appears to be challenging and not well understood.

To this end, the main contributions of this research are twofold. First, a general AAAC model is proposed for reasoning about different ways of controlling approximation errors and present optimal error compensation schemes under ideal design scenarios. The proposed model is general in the sense that it captures the key design structure that is common to a major class of array-based approximate arithmetic units (*e.g.*, multipliers, squarers, dividers, adders/subtractors and logarithmic function units). The proposed model offers critical insights of optimized error compensation schemes and the corresponding signatures generation logic that is the key to error compensation.

Second, as two specific applications, by leveraging the design insights obtained from the proposed model, this thesis presents a new approximate Booth multiplier and squarer design that achieve noticeable reduction of error compared with existing designs while maintaining significant benefits in terms of delay, area and energy consumption due to the approximate nature of computation.

The proposed approximate 16-bit fixed-width Booth multiplier consumes 44.85% and 28.33% less energy and area compared with theoretically the most accurate fixed-width Booth multiplier. Furthermore, it reduces average error, max error and mean square error by 11.11%, 28.11% and 25.00%, respectively, when compared with the best reported approximate Booth multiplier and outperforms the best reported approximate design significantly by 19.10% in terms of the energy-delay-mean square error product

(EDE_{ms}). For the proposed approximate 16-bit fixed-width squarer, a 18.18%, 21.67% and 31.25% reduction is achieved on average error, max error and mean square error, respectively. Furthermore, EDE_{ms} is improved by more than 20.00%, when compared with existing designs. By utilizing extra signatures and don't cares, the energy-delay-max error product (EDE_{max}) is further reduced by 15.81% for the proposed 16-bit fixed-width squarer. Additionally, when operated in the full-width mode, the proposed multiplier and squarer have an even greater improvement of accuracy.

1.2 Previous work

1.2.1 Approximate multipliers

As mentioned in Sub-section 1.1, there are mainly two types of approximate multipliers existing: approximate AND-array multipliers, which utilize AND gates for partial products generation and approximate Booth multipliers, which use the modified Booth algorithm to reduce the number of partial products. Constant correction [1] and variable correction [2] schemes are proposed for approximate AND-array multipliers. Constant correction scheme suggests adding one constant to compensate for the truncated error and variable correction multipliers add some signals in the partial product table to make compensation.

However, since Booth multipliers are much more efficient than AND-array multipliers, approximate Booth multipliers have been intensively investigated [3]-[8]. In particular, statistical linear regression analysis [3], estimation threshold calculation [4] and self-compensation approach [5] have been utilized to compensate the truncation error. Accuracy is increased by using certain outputs from Booth encoders [6] [7]. To

decrease energy consumption, a probabilistic estimation bias (PEB) scheme [8] is presented.

1.2.2 Approximate squarers

A series of approximate squarers have been proposed [9]-[11]. For instance, the designs of [9] and [10] compensate truncation error by utilizing constant and variable correction scheme, respectively. A LUT-based squarer [11] is proposed by employing a hybrid LUT-based structure.

2. ARRAY-BASED APPROXIMATE ARITHMETIC COMPUTING (AAAC) MODEL

Fig. 1 contrasts an Error-Free Computing Unit (EFCU) with n -bit inputs and an m -bit output (a) with its approximate counterpart modeled using the proposed AAAC model (b). The AAAC model consists of three units: Low-Precision Computing Unit (LPCU), Error Compensation Unit (ECU) and Combine Unit (CU).

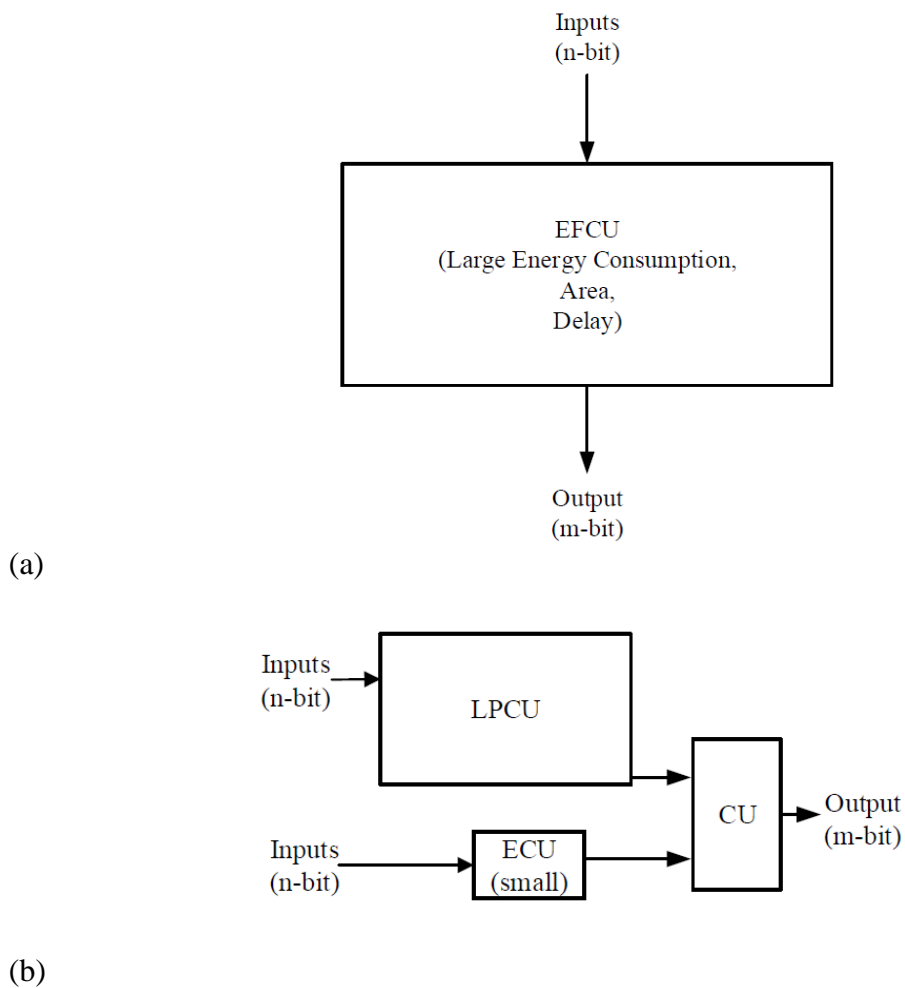


Figure 1. Arithmetic computing unit models: (a) Error-Free Computing Unit (EFCU) model (large energy consumption, area and delay), (b) Proposed AAAC model (small energy consumption, area and delay).

The LPCU in the AAAC circuit produces a low-precision approximate output, for example, based upon truncation or a fraction of the input bits, with lowered energy, delay and/or area overheads compared with the error-free EFCU.

To reduce the error produced by the LPCU, a low-cost ECU may be included for error comparison. Finally, the CU combines the error compensation produced by the ECU with the result outputted by the LPCU, generating the final output of the AAAC unit with reduced approximate error.

The *generality* of the AAAC model lies in the fact it reflects the key computing principles behind a wide range of array-based arithmetic units, for example, approximate adders [12]-[14], approximate multipliers [1]-[8] and approximate squarers [9]-[11]. For instance, many approximate adders employ carry prediction from low input bits, which can be thought as a particular way of implementing the ECU. Similarly, error compensation is a common scheme in approximate multipliers and squarers.

Clearly, the key AAAC design problem is to develop an efficient LPCU and, in particular, an ECU so as to significantly reduce energy, delay and/or area overhead while achieving a low degree of approximation error. While the area and energy of a given design can often be easily reasoned or estimated, the key challenge is to develop insights on error or error distribution so as to optimize the error compensation scheme, which is focused on in the following sections.

2.1 Error Metrics

This research evaluates a given AAAC design with n -bit inputs by defining average error E_{ave} , maximum error E_{max} and mean square error E_{ms} , respectively as

$$E_{ave} = \frac{1}{2^n \cdot N} \sum_{i=1}^N |O_{AAAC,i} - O_{EFCU,i}| \quad (1)$$

$$E_{max} = \frac{1}{2^n} \max_i |O_{AAAC,i} - O_{EFCU,i}| \quad (2)$$

$$E_{ms} = \frac{1}{2^{2n} \cdot N} \sum_{i=1}^N (O_{AAAC,i} - O_{EFCU,i})^2 \quad (3)$$

where N , $O_{AAAC,i}$ and $O_{EFCU,i}$ denote the number of all possible input combinations, output of the AAAC, and output of EFCU (error-free result), respectively, for each input combination i . Note that the above error metrics are normalized with respect to the range of the output 2^{2n} .

As shown in Fig. 1 (b), for each input combination i , the ECU outputs error compensation, denoted by $Comp_i$. Hence the output of the AAAC circuit is: $O_{AAAC,i} = O_{LPCU,i} + Comp_i$, where $O_{LPCU,i}$ is the output of the LPCU. Importantly, the error of the LPCU, i.e., the error of the AAAC before compensation ($E_{BC,i}$) and after compensation ($E_{AC,i}$) is given simply by

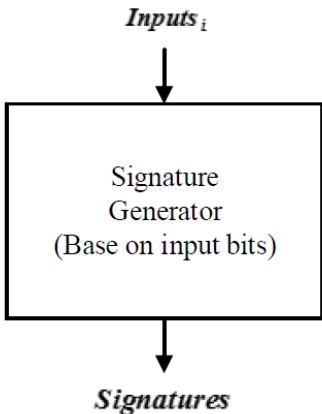
$$E_{BC,i} = O_{EFCU,i} - O_{LPCU,i} \quad (4)$$

$$E_{AC,i} = |E_{BC,i} - Comp_i| \quad (5)$$

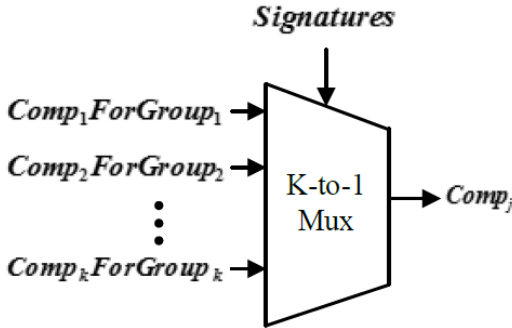
2.2 Model of Error Compensation Unit (ECU)

Ideally, a specific $Comp_i$ can be computed by the ECU to perfectly zero out the error for each input pattern i . However, this does not serve any purpose for approximate computing as we are essentially re-implementing the error-free operation. We present a practical yet general ECU model, which consists of a Signature Generator (a) and a K-to-1 Mux (b), as shown in Fig. 2. Conceptually, for a given input pattern i , the signature generator produces several signatures that encode certain essential information about the

inputs. Based on the actual values of the extracted signatures, this input pattern is classified into one of the K predetermined input classes with each having a predetermined error compensation $Comp_j$ ($j = 1, 2, \dots, K$). The compensation for this input pattern is produced by using the signature values to select the constant compensation of its corresponding input group via the K -to-1 mux.



(a)



(b)

Figure 2. ECU model: (a) Signature generator, (b) Fixed compensation per input group.

It is important to note that the structure of the ECU model may not immediately correspond to the specific logic implementation of the ECU. Nevertheless, it captures the general working principle of error compensation for AAAC.

2.3 Ideal Error Compensation & ECU Design

To shed light on the ECU according to the proposed model, we visualize the classification of the input space based on the chosen signature for the case of two inputs in Fig. 3, where the input groups may overlap. In the extreme case, if each input group has only one input pattern, then the optimal compensation for each group/input would be simply the corresponding $E_{BC,i}$ (eqn. 4). However, in practical cases, we would need to consider the $E_{BC,i}$ distribution within each group.

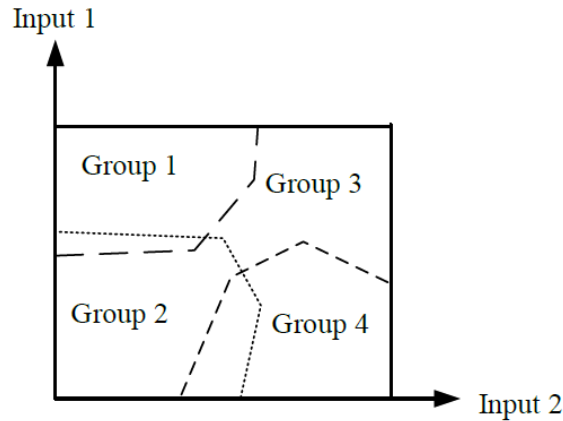


Figure 3. Classification of the inputs based on the signatures.

Now it is evident that the key ECU design problem is to find an optimal signature generation scheme that minimizes one or more error metrics (i.e., E_{ave} , E_{max} and E_{ms}) under a given set of cost constraints (e.g., area, delay and energy). Note that the cost of

the ECU often strongly correlates with the number of input groups K . We show several provable results for optimal selection of error compensation constants for a given compensation scheme. We also show an optimal error compensation scheme under an ideal scenario with specific illustration for each. We first denote the number of input patterns that fall in the j^{th} group by N_{G_j} .

Theorem 1: *The optimal error compensation $Comp_j$ for the j^{th} group that minimizes E_{ave} is the median of $E_{BC,i}$ (eqn. 4) of the group if N_{G_j} is odd; otherwise it can be any value that falls in the inclusive interval between the two medians of $E_{BC,i}$.*

For j^{th} group, minimizing E_{ave} leads to minimization of the sum of distances from each $E_{BC,i}$ to $Comp_j$, which makes the value of $Comp_j$ the median of $E_{BC,i}$ of the group if N_{G_j} is odd. On the other hand, when N_{G_j} is even, $Comp_j$ can be any value that falls in the inclusive interval between the two medians of $E_{BC,i}$.

Theorem 2: *The optimal error compensation $Comp_j$ for the j^{th} group that minimizes E_{max} is the mean of $E_{BC,min}$ and $E_{BC,max}$, where $E_{BC,min}$ and $E_{BC,max}$ are the minimum and maximum values of $E_{BC,i}$ in the group, respectively.*

Assume that $E_{BC,min}$ and $E_{BC,max}$ are the minimum and maximum values of $E_{BC,i}$ in the group. We have $h = (E_{BC,max} - E_{BC,min})/2$ is the minimum E_{max} value that can be achieved when $Comp_j$ is the mean of $E_{BC,min}$ and $E_{BC,max}$. Otherwise, either $(Comp_j - E_{BC,min})$ or $(E_{BC,max} - Comp_j)$ is greater than h .

Theorem 3: *The optimal error compensation $Comp_j$ for the j^{th} group that minimizes E_{ms} is the mean of all $E_{BC,i}$ in this group.*

To see how Theorem 3 may be proven, consider the j^{th} group, for which we have

$$E_{ms} = \sum_{i=1}^{N_{G_j}} (E_{BC,i} - Comp_j)^2 / N_{G_j} \quad (6)$$

To minimize E_{ms} , let $\frac{\partial E_{ms}}{\partial Comp_j} = 0$, we have

$$Comp_j = \sum_{i=1}^{N_{G_j}} E_{BC,i} / N_{G_j} \quad (7)$$

Eqn. 7 indicates that to minimize E_{ms} for one group, the best compensation is the average of all $E_{BC,i}$ in this group.

The above three theorems suggest the following important design guidance. For a given compensation scheme, the compensation $Comp_j$ for each input group can be optimally determined according to the results above to minimize the targeted error metric.

Now we turn into the other design problem by presenting the optimal error compensation scheme under an ideal scenario.

Theorem 4: *Assume that $E_{BC,i}$ is uniformly and continuously distributed from $\bar{E}_{BC,min}$ to $\bar{E}_{BC,max}$, where $\bar{E}_{BC,min}$ and $\bar{E}_{BC,max}$ are the minimum and maximum values of $E_{BC,i}$, in the entire input range, then the optimal E_{ms} -minimizing error compensation scheme with K input groups partitions the entire $E_{BC,i}$ range into K non-overlapping equal-length intervals with one interval corresponding to a specific input group.*

To set some intuition of the theoretical result presented in Theorem 4, let us consider a 4-group example. Assume DS_1, DS_2, DS_3, DS_4 and DS_5 are bounds of four non-overlapped groups on the $E_{BC,i}$ axis, where $DS_1 < DS_2 < DS_3 < DS_4 < DS_5$, as

shown in Fig. 4. DS_1 and DS_5 are the lower and upper bound of all $E_{BC,i}$ and fixed when input cases are given. E_{ms} can be written as

$$E_{ms} = \left[\int_{DS_1}^{DS_2} (E_{BC,i} - Comp_j)^2 dE_{BC,i} + \int_{DS_2}^{DS_3} (E_{BC,i} - Comp_j)^2 dE_{BC,i} + \int_{DS_3}^{DS_4} (E_{BC,i} - Comp_j)^2 dE_{BC,i} + \int_{DS_4}^{DS_5} (E_{BC,i} - Comp_j)^2 dE_{BC,i} \right] / (DS_5 - DS_1),$$

where to minimize E_{ms} , according to Theorem 3, the optimal compensation for the j^{th} group is given by $Comp_j = (DS_j + DS_{j+1})/2$. Then, let $\frac{\partial E_{ms}}{\partial DS_j} = 0$ ($j = 2, 3, 4$), we have

$$DS_3 - DS_2 = DS_2 - DS_1$$

$$DS_4 - DS_3 = DS_3 - DS_2$$

$$DS_5 - DS_4 = DS_4 - DS_3$$

Therefore,

$$DS_2 - DS_1 = DS_3 - DS_2 = DS_4 - DS_3 = DS_5 - DS_4 \quad (8)$$

Eqn. 8 indicates that the four input groups are non-overlapping and in equal length. Note that $E_{BC,i}$ is discrete and hence not continuously distributed in reality. This continuous assumption is a good approximation when the error is densely populated between $\bar{E}_{BC,\min}$ and $\bar{E}_{BC,\max}$.

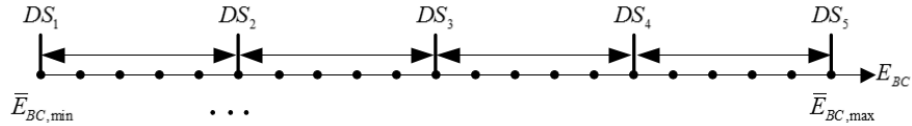


Figure 4. A 4-group example for Theorem 4.

2.4 Further Reduction of Error and Cost

In practice, the above theoretical results can be used to come up with a good error compensation scheme and the corresponding optimal compensation value for each input group while considering logic implementation complexity. For a given application, this process may help us identify a highly compact set of signatures. With a good initial set of signatures chosen, to further reduce error, one effective way may be to add extra signatures by directly considering certain input bits. Such signatures can further divide the K predetermined input classes into groups with each group having a predetermined error compensation. For example, seven input bits might be chosen as extra signatures to sub-divide each of the K predetermined classes into 128 groups.

Considering about logic complexity, if the compensations for all the groups are implemented precisely, an ECU with a complex logic will be generated through logic synthesis, though the error may be minimized. Therefore, tradeoff between logic complexity and error should be made. In order to simplify ECU design, we can set compensation values of some groups which don't contribute much of the overall error to be don't cares so that the overall error won't be increased dramatically.

According to the principle of logic synthesis [15], don't care set may contribute significantly for logic minimization. Specifically, the groups whose compensations not set to be don't cares belong to on-set (contains all input cases leading to output '1') and those set to be don't cares belong to dc-set (don't care set, contains all input cases leading to output "don't care"). Standard logic synthesis algorithms such as Quine-McCluskey Algorithm [15] calculate all prime implicants of the union of the on-set and

dc-set, omitting prime implicants that only cover points of the dc-set, and finds the minimum cost cover of all minterms in the on-set from the obtained prime implicants. Clearly, the dc-set helps simplify the resulting logic.

It's necessary to mention how we set don't cares in Verilog HDL. In logic synthesis, don't cares can be expressed using special non-Boolean values, such as 'x' [16]. When having the design synthesized by synthesis tools such as Synopsis Design Compiler [17], we set constraints of minimizing power (both dynamic and leakage power) and area, so an optimal logic will be generated through logic synthesis. In this way, we are able to simplify the design with the help of synthesis tools by setting some groups to be don't cares.

The method of introducing don't cares for designs in Verilog HDL is shown in the following example. If power (both dynamic and leakage power) constraints and area constraint are set to Synthesis Tools such as Synopsis Design Compiler [17], to simplify the logic and minimize power and area, when *In* is "0001", "0010", "1001" or "1010", *Out* is set to be '1' in these four cases, so the overall logic becomes

$$Out = \overline{In[3] \cdot In[2] \cdot In[1] \cdot In[0]}$$

which generates the simplest logic. Otherwise, the logic will be much more complex, thus consuming more power and area accordingly.

//An example of introducing don't cares in Verilog HDL

//In: 4-bit variable

//Out: 1-bit variable

Case (In) is

When “0000” => Out = ‘1’

When “0001” => Out = ‘x’

When “0010” => Out = ‘x’

When “0011” => Out = ‘1’

When “0100” => Out = ‘1’

When “0101” => Out = ‘1’

When “0110” => Out = ‘1’

When “0111” => Out = ‘1’

When “1000” => Out = ‘1’

When “1001” => Out = ‘x’

When “1010” => Out = ‘x’

When “1011” => Out = ‘1’

When “1100” => Out = ‘1’

When “1101” => Out = ‘1’

When “1110” => Out = ‘1’

When “1111” => Out = ‘0’

End Case

//End example

The issue now becomes how to determine which groups should be given high priority to be set as don't cares. We come up with an idea to rank all the groups based on their impact on the target error metric when set to be don't cares. For example, when targeting on minimizing E_{max} of a given group, we rank all the groups by the greatest

value of E_{max} because the compensation value which is the output of a group can be assigned to be any value of a specific range for logic complexity simplification when set to be don't cares. Then, the groups which have smaller greatest E_{max} are given higher priority to be set as don't cares, while other groups are implemented precisely because they have comparatively larger E_{max} .

2.5 Practical ECU Design Guidance

The above theoretical analysis provides optimal design strategies for minimizing a particular error metric. In practice, minimization of one error metric may often lead to near-optimal minimization of other error metrics. We summarize the practical ECU design guidance that is directly resulted from these results:

- 1) Different input groups shall have no or little overlap on the $E_{BC,i}$ axis to minimize approximation error;
- 2) The $E_{BC,i}$ spread of each group shall be largely of equal length;
- 3) Non-uniformity of $E_{BC,i}$ spread may be reduced by splitting groups with a large spread into smaller groups;
- 4) For a given compensation/grouping scheme, the optimal compensation values for all groups can be determined to minimize a given error metric according to Theorems 1-3.
- 5) Better accuracy performance can be achieved by introducing extra signatures of certain input bits to divide large classes into small groups with different compensation value for each group. Energy consumption and area can be

further reduced by introducing don't cares to some of the groups which have comparatively small impact on the overall error.

3. PROPOSED MULTIPLIER DESIGN

The AAAC model is applied to approximate fixed-width Booth multiplier design and its extension to full-width multipliers.

3.1 Fundamentals of Booth Multipliers

Booth multipliers are ideal for high speed applications and the Radix-4 Modified Booth multipliers are most widely applied [18] [19]. The main blocks of a Radix-4 Modified Booth multiplier are shown in Fig. 5. The encoding block applies the Radix-4 Booth Algorithm to encode the multiplier B, allowing the selection block to generate only half number of partial products needed for array multipliers with each partial product being one of the following: 0, A, 2A, -A, -2A. Then, the compressors in the compression block compress the number of partial products to two [20] [21]. Finally, a 2n-bit adder is used to generate the final product.

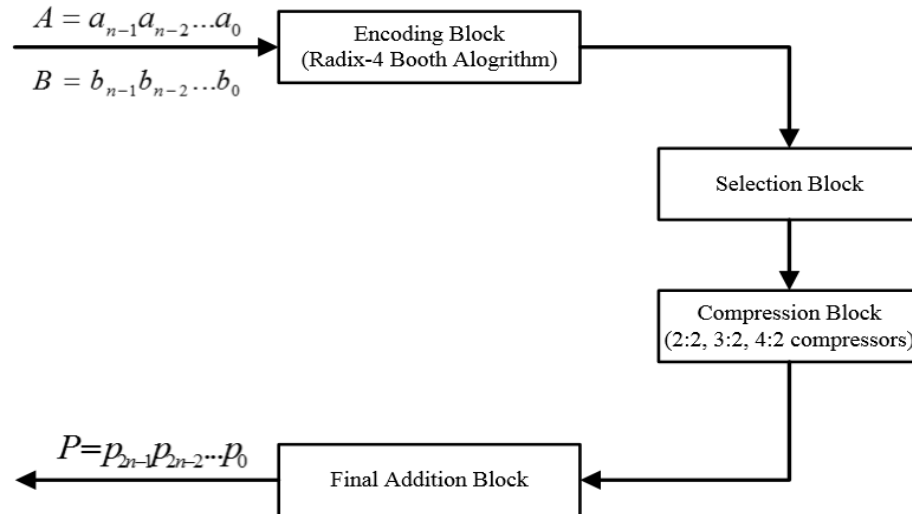


Figure 5. Error-Free Booth multiplier blocks.

3.2 The Basic Idea

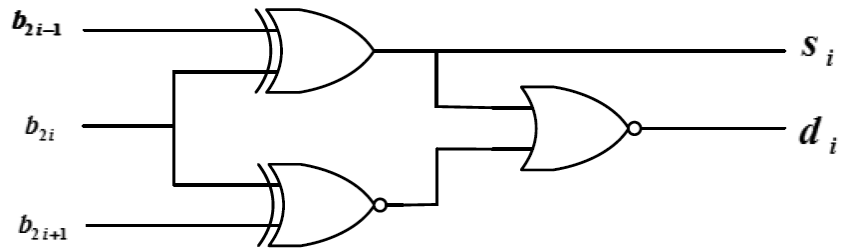
In this work, we use $n \times n$ fixed-width Booth multipliers to refer to approximate Booth multipliers that operate on two n -bit inputs while outputting only an n -bit product [4]. For convenience of discussion, we assume the higher and lower n bits of the multiplicand and multiplier correspond to the integer and fractional parts of the inputs, respectively. In this regard, a fixed-width multiplier outputs, possibly in an approximate manner, the n -bit integer part of the exact product.

Fig. 6 shows the schematics of Radix-4 Booth encoding block applied in this research, the outputs of encoding block are s_i , d_i , n_i , z_i and c_i : (a) is the schematic of s_i , d_i generation. (b) is the schematic of n_i generation. (c) is the schematic of z_i generation. (d) is Schematic of c_i generation.

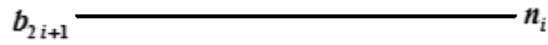
z_i signifies whether the partial product is zero or not, n_i specifies the sign of each partial product, $\{d_i, s_i\}$ determines magnitude of the value multiplied by A for the partial product (0, A or 2A), where d_i is the more significant bit and s_i is the less significant bit. c_i is the correction constant required to generate the negative partial product.

s_i , d_i , n_i , z_i and c_i are generated by three consecutive input bits of multiplier B, which are b_{2i-1} , b_{2i} and b_{2i+1} .

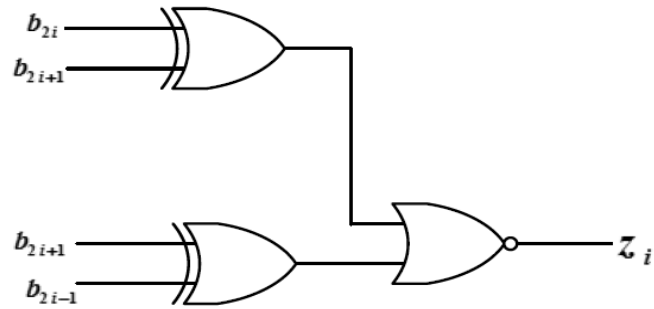
Fig. 7 presents the schematic of the selection block applied in this research, where $pp_{i,j}$ represents the j^{th} bit of i^{th} partial product.



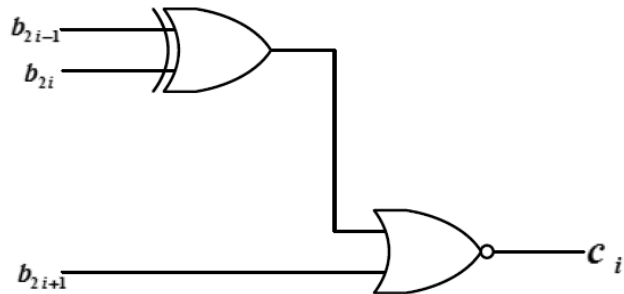
(a)



(b)



(c)



(d)

Figure 6. Schematics of Radix-4 Booth encoding block: (a) Schematic of s_i , d_i generation, (b) Schematic of n_i generation, (c) Schematic of z_i generation, (d) Schematic of c_i generation.

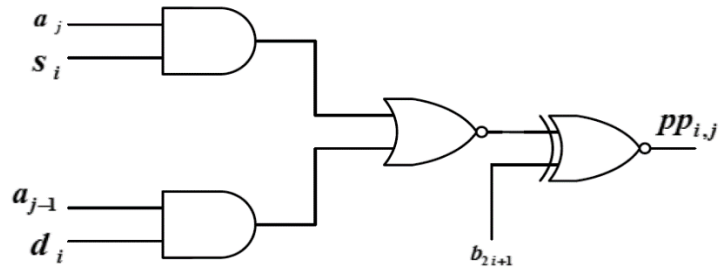


Figure 7. Schematic of the selection block.

Fig. 8 shows the full 8-partial product array for a full-precision 16x16 bits Booth multiplier where each dot row (PP_0 to PP_7) is a partial product. The 16 dots (bits) in each PP_i are denoted by $pp_{i,15}pp_{i,14}\dots pp_{i,10}$ from left to right. The vertical dashed line splits the array at the position of the binary (radix) point. A fixed-width multiplier outputs an integer output by approximating the carry-out produced by the fractional part of the array, which is also labeled as the truncation part (TP). On the other hand, the contribution of the bits left of the binary point, *i.e.*, ones in the accurate part (AP), is not approximated.

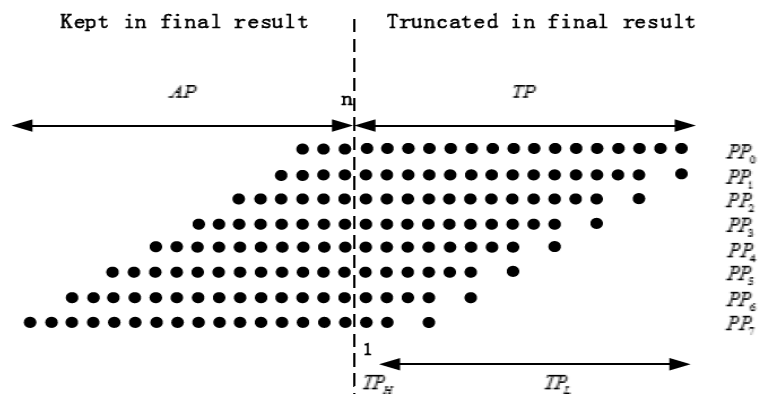


Figure 8. Partial product diagram for fixed-width 16x16 bits Booth multipliers (n=16).

Direct-Truncated Booth multipliers (DTM) [5], which are an extreme case of fixed-width multipliers, output an n -bit integer product by simply neglecting the bits in the TP part of the array without forming them in the first place, thus potentially producing a large error. As another extreme, Post-Truncated Booth multipliers (PTM) [3] form the complete partial product array, compress all the bits, compute with full precision, add an extra “1” to the $n - 1^{th}$ column to exactly round the carry-out to the n^{th} column, and finally output the exact n -bit integer part of the final product (with rounding), as shown in Fig. 8. As such, PTMs are the most accurate fixed-width multipliers.

Our goal in approximate fixed-width multiplier design is to approach the accuracy of a PTM without incurring its high overhead that is commensurate with that of a full-precision multiplier. Under the AAAC model, we associate the accurate part (AP) and the truncation part (TP) of the array in Fig. 8 with the LPCU and ECU, respectively. More specifically, the bits in AP are processed by the LPCU while the effects of the ones in TP are approximated by the ECU in the form of error compensation. The exact product (EFCU output) is

$$O_{EFCU} = O_{LPCU} + S_{TP}$$

where S_{TP} is the partial sum of TP, and O_{LPCU} is the LPCU output corresponding to AP. To reduce the amount of approximate error, we further divide TP into TP_H (*i.e.*, the $n - 1^{th}$ column) and TP_L and have

$$S_{TP,H} = \frac{1}{2}SUM_{n-1}$$

$$S_{TP,L} = \frac{1}{4}SUM_{n-2} + \frac{1}{8}SUM_{n-3} + \dots + \left(\frac{1}{2}\right)^n SUM_0 \quad (9)$$

where $S_{TP,H}$ and $S_{TP,L}$ correspond to the partial sums of TP_H and TP_L , and SUM_i represents the sum of all bits in the i^{th} column, respectively. Now it is clear that

$$S_{TP} = S_{TP,H} + S_{TP,L}$$

The main objective in the design of ECU is to well approximate

$$S_{TP} \approx O_{ECU}$$

such that a fixed-width n-bit output is produced, *i.e.*,

$$O_{EFCU} = O_{LPCU} + S_{TP} \approx O_{LPCU} + O_{ECU}$$

Note again that the ECU of a PTM (most accurate fixed-width multiplier) produces as the output (with rounding)

$$O_{ECU,PTM} = \text{int}(S_{TP} + 1) = \text{int}(S_{TP,H} + S_{TP,L} + 1) \quad (10)$$

where $\text{int}(\cdot)$ returns the integer part of its argument. To approach the PTM, we design our ECU's output to be

$$O_{ECU} = \text{int}(S_{TP,H} + \widetilde{S_{TP,L}} + 1) \quad (11)$$

where $\widetilde{S_{TP,L}}$ is a good approximation to $S_{TP,L}$. In (11), only $\widetilde{S_{TP,L}}$ is approximated by the ECU while $S_{TP,H}$ is computed exactly. Regarding to (11), we denote the carry-out from TP_L to TP_H by θ

$$\theta = \text{int}(2 \cdot S_{TP,L}) \quad (12)$$

(10) can now be simplified to

$$O_{ECU,PTM} = \text{int}(S_{TP,H} + \frac{1}{2}\theta + 1) \quad (13)$$

Going back to (11), it is now clear that the main task of the ECU design is to well approximate θ . Since $S_{TP,H}$ is kept exact in (11), it is also natural to associate both AP and $S_{TP,H}$ with the LPCU, and process them with the LPCU's encoding and selection blocks. In this case, the ECU only produces an approximate θ .

3.3 Design of Error Compensation Unit

According to Section 2.5, the key problem in the ECU design is to classify all input patterns into largely equally sized groups with none or little overlap according to values of $E_{BC,i}$, which is the error before compensation (in this case θ).

To start, we first examine the standard Booth encoding that encodes each set of three consecutive bits of multiplier B into five signals and determines the corresponding partial product in terms of multiplicand A in Table 1, where z_i signifies whether the partial product is zero or not, n_i specifies the sign of each partial product, $\{d_i, s_i\}$ determines magnitude of the value multiplied by A for the partial product (0, A or 2A), c_i is the correction constant required to generate the negative partial product and added to the end of the partial product and PP_i is the actual i^{th} partial product generated from the selection block.

As in Fig. 8, it is worth noting that Booth encoding is applied across the entire partial product array including the TP part, which is associated with the error.

By following the ECU design guidance in Section 2.5, we identify a set of error compensation signatures of low cost from Table 1, which shows signals of Radix-4 Booth encoding, to compensate for the error due to TP.

Input bits of Multiplier B (for i^{th} partial product)			Booth Encoder Outputs (for i^{th} partial product)					Partial Product
b_{2i+1}	b_{2i}	b_{2i-1}	z_i	c_i	n_i	d_i	s_i	PP_i
0	0	0	1	0	0	0	0	0
0	0	1	0	0	0	0	1	A
0	1	0	0	0	0	0	1	A
0	1	1	0	0	0	1	0	2A
1	0	0	0	1	1	1	0	-2A
1	0	1	0	1	1	0	1	-A
1	1	0	0	1	1	0	1	-A
1	1	1	1	0	1	0	0	0

Table 1. Signals of Radix-4 Booth encoding.

Our key idea is to use encoded sign and magnitude information of the partial products to classify the input patterns into largely equally sized non-overlapping groups according to the $E_{BC,i}$ value. In the following, we first present a set of error signatures for each partial product, and then compress them for the entire ECU.

- 1) The first signature to be chosen is z_i . It is effective since a non-zero value of z_i signifies the zero-valued corresponding partial product PP_i , thereby classifying the inputs into two $E_{BC,i}$ (zero vs. non-zero error) groups independently of the multiplicand A.

Starting from these two input groups, we select our second signature to be n_i , which encodes the sign of PP_i , allowing us to further partition the large non-zero $E_{BC,i}$ input group into two smaller groups of positive vs. negative error.

To further reduce the approximation error, we introduce the third signature to split the large signed error input groups by using the magnitude

information of each partial product. For this, we count the number of non-zero bits in multiplicand A

$$n_{nza} = \sum_{i=0}^{n-1} a_i$$

- 2) Note that n_i and z_i are defined for each partial product and there are $n/2$ partial products for $n \times n$ bits multiplication. In addition, n_{nza} ranges from 0 to n . Utilizing these signatures for the ECU would create a huge number of input groups and lead to significant area and energy overhead. To simplify the design of the signature generator, we first sum up n_i and z_i to produce CA and CB, respectively, and then introduce a Boolean variable FA that indicates whether n_{nza} is above $n/2$ or not

$$\begin{aligned}
 CA &= \sum_{i=0}^{\frac{n}{2}-1} z_i \\
 CB &= \sum_{i=0}^{\frac{n}{2}-1} n_i \\
 FA &= \begin{cases} 0, & \sum_{i=0}^{n-1} a_i < \frac{n}{2} \\ 1, & \sum_{i=0}^{n-1} a_i \geq \frac{n}{2} \end{cases} \quad (14)
 \end{aligned}$$

CA, CB and FA are the final set of compressed signatures we use for the ECU. These signatures can be implemented with low-cost in hardware. Fig. 9 illustrates the design of the proposed signature generator that consists of two carry propagation adders (CPAs) for generating CA, CB and an n -input odd-even sorting network [22] (Fig. 10) for FA

generation. Note that n_i and z_i are already computed by the encoders in the LPCU.

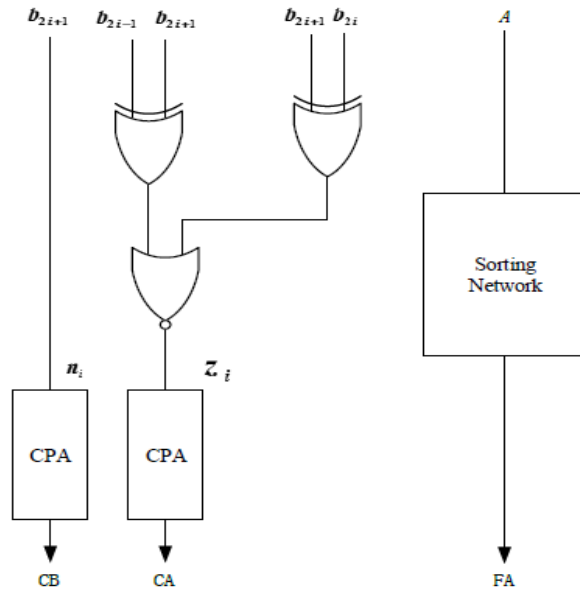


Figure 9. Blocks and schematics of Signature Generator.

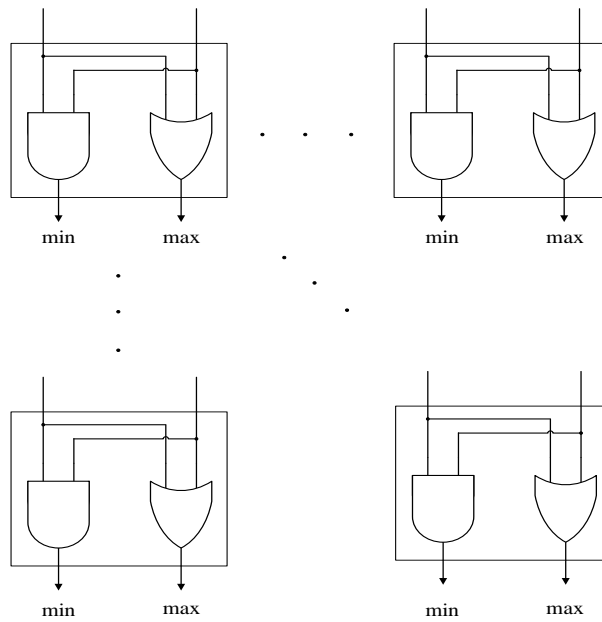


Figure 10. Blocks of sorting network.

3.4 The Complete Fixed-Width Multiplier

With the selected signatures and classified input groups, next, we need to determine the actual error compensation for each group, *i.e.*, an approximate to θ in (12). As discussed in Section 2.3, one can follow Theorems 1-3 to choose a fixed compensation for each input group to minimize a targeted error metric. For example, to minimize E_{ms} , the optimal compensation is the average $int(2 \cdot S_{TP,L})$ value for each group. The ECU is designed to run in parallel with the selection block and part of compression block so that it causes little extra delay during runtime.

We take 16x16 bits fixed-width Booth multiplier design as an example to illustrate the signature and compensation generation schemes, and additional possible simplifications. To further simplify the ECU, we consider different ranges and combinations of the signature values in Table 2, where \wedge denotes AND operation. In Table 2, the conditions of five cases are mainly determined by CA.

For CA in range [0, 1], when $(CA = 1) \wedge (CB < 3) \wedge (FA = 0)$, the corresponding input patterns belong to Case 1. The rest of input patterns when CA in range [0, 1] belong to Case 2.

For CA in range [2, 5], when $(CA = 2) \wedge (CB > 3) \wedge (FA = 0)$ or $(CA = 2) \wedge (CB < 3) \wedge (FA = 1)$, the corresponding input patterns belong to Case 3. The rest of input patterns when CA in range [2, 5] belong to Case 4.

For CA in range [6, 8], all input patterns belong to Case 5.

The goal is to identify a smaller set of refined input groups with controlled error spread. $\bar{S}_{TP,L}$ is the average of $S_{TP,L}$ in each input group.

Case	$\bar{\theta}$	$\bar{S}_{TP,L}$
1	1	0.9853
2	2	1.1259
3	2	1.0188
4	1	0.8580
5	0	0.4001

Table 2. Compensation for input groups of 16x16 multiplier.

To minimize E_{ms} , the optimal integer error compensation $\bar{\theta}$ is set to be the average of (8) in the group.

To further simplify, as shown in Table 3, the cases which have the same $\bar{\theta}$ are merged into the same group. Therefore, Case 2 and Case 3 are merged to form Group 1 (G1). Group 2 (G2) consists of Cases 1 and 4. Finally, Case 5 forms Group 3 (G3). Each merged group has the same $\bar{\theta}$ (average compensation value for all input cases in one group) and error selection is realized by a simple 3-to-1 mux.

Group Number	Case Number	$\bar{\theta}$	$\bar{S}_{TP,L}$
1	2, 3	2	1.1153
2	1, 4	1	0.8608
3	5	0	0.4001

Table 3. Optimal compensation for the refined input groups.

3.5 Proposed Full-Width Booth Multiplier

Approximate full-width multipliers, *i. e.*, ones that approximate accurate $n \times n$ Booth multipliers by outputting a full-width $2n$ -bit approximate product, are also useful for many practical applications.

The presented fixed-width design can be readily extended to facilitate full-width operation with the difference being that in this case we would like to approximate $S_{TP,L}$ by $\widetilde{S}_{TP,L}$ as in (11).

Again, to minimize E_{mS} , for instance, the optimal compensation for each input group would be the average of $S_{TP,L}$, denoted by $\bar{S}_{TP,L}$, in that group. For $n=16$, we show the values of $\bar{S}_{TP,L}$ for the same three input groups in the last column of Table 3.

4. PROPOSED SQUARER DESIGN

4.1 The Basic Squarer Design

We demonstrate the application of the AAAC model to approximate fixed-width squarers and its extension to full-width squarer designs.

Fig. 11 shows the full 8-partial squaring array (PS_0 to PS_7) for a full-precision 16-bit squarer, where the input is denoted by $A(a_{n-1} \dots a_0)$ [9].

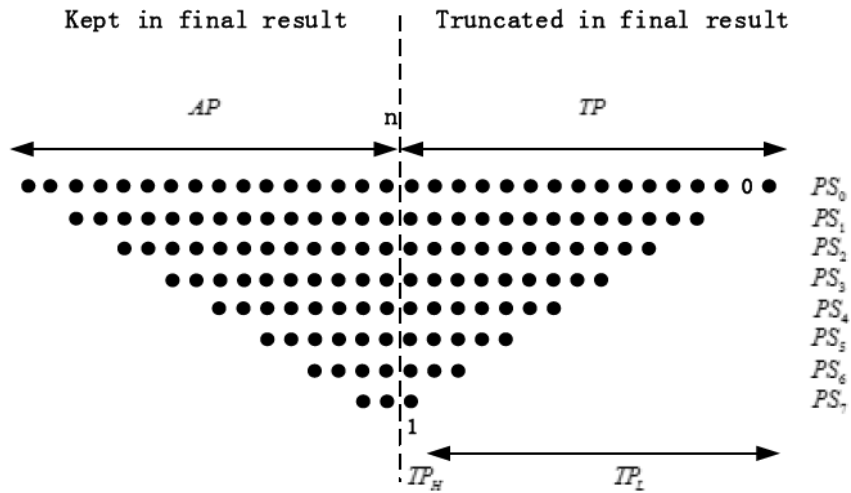


Figure 11. Squaring diagram for 16-bit fixed-width squarers.

Here, we use the method in [9] to implement squarers instead of using Booth algorithm as applied to multiplier design in Section 3 [9] because squarers implemented by using the method in [9] are more energy-efficient and faster since most partial products bits are implemented by simple AND operation of two input bits instead of more complex Booth encoding and selection blocks.

The squarer design process is similar to the one presented for the proposed multipliers (*e.g.*, based on eqn. (9 - 13). Again, the key problem is to design an ECU to well approximate θ . By following the ECU design guidance in Section 2.5, we consider the signals on the $n - 2^{th}$ column as signatures since they have the highest weight on TP_L and include all input bits which contribute to TP_L .

To simplify the design of the signature generator, we sum up the signals on the $n - 2^{th}$ column to produce the first signature CA. We introduce one input bit as the second signature (CB) to further split the large input groups formed by CA. Accordingly, input bit a_6 is chosen as the second signature CB for the proposed 16-bit squarer.

The final input cases of the 16 bit squarer classified by CA and CB are show in Table 4. CA is generated by an odd-even sorting network [22], which has a low hardware overhead, and CB is selected directly from the input A. The error compensations $\bar{\theta}$ for the fixed-width squarer are shown in the second last column of Table 4. The values of $\bar{S}_{TP,L}$ (error compensation) of different input cases for the full-width squarer are shown in the last column of Table 4.

Case	Condition	$\bar{\theta}$	$\bar{S}_{TP,L}$
1	$CA = 0$	0	0.2197
2	$(CA = 1) \wedge (CB = 0)$	0	0.4539
3	$(CA = 1) \wedge (CB = 1)$	1	0.6210
4	$(CA = 2) \wedge (CB = 0)$	1	0.8133
5	$(CA = 2) \wedge (CB = 1)$	2	1.0134
6	$CA = 3$	2	1.2902
7	$CA = 4$	3	1.6966
8	$CA = 5$	4	2.1278
9	$CA = 6$	5	2.5838
10	$CA = 7$	6	3.0645

Table 4. Compensation for input cases of 16-bit squarer.

According to $\bar{\theta}$ in different input cases, for 16-bit fixed-width squarer design, we combine them into seven groups, which are shown in Table 5. Case 1 and case 2 are merged to group 1. Case 3 and Case 4 form group 2. Group 3 consists of case 5 and case 6. Then case 7 becomes group 4, case 8 becomes group 5, case 9 becomes group 6 and finally, case 10 becomes group 7.

Group	Case	$\bar{\theta}$
1	1, 2	0
2	3, 4	1
3	5, 6	2
4	7	3
5	8	4
6	9	5
7	10	6

Table 5. Compensation for input groups of 16-bit squarer.

4.2 Further Error and Cost Reduction for Fixed-Width Squarers

As described in Section 2.4, we may introduce extra signatures of certain input bits to sub-divide each of the large input classes into groups to further reduce one or more error metrics. To further simplify the logic, thus decreasing energy consumption and area of ECU after introducing extra signatures, don't cares are added for certain input groups.

Now we introduce extra signatures and don't cares to further decrease E_{max} as well as energy consumption and area for the proposed 16-bit fixed-width squarer. To give an overall evaluation of designs, an energy-delay-max error product is defined as $Energy \cdot Delay \cdot E_{max}$ (EDE_{max}).

First, we introduce extra input signatures. In the proposed 16-bit fixed-width squarer design, input bit a_6 is utilized as one signature because it can further divide some of the large eight classes formed by signature CA into groups. Specifically, we try each input bit from a_0 to a_{15} according to the design guidance in Section 2 that an efficient signature should be able to divide input cases into groups largely of equal length (sub-dividing large input classes formed by the first signature CA in this case). The simulation results indicate that selecting a_6 as a signature can divide more large original groups formed by the first signature CA and achieve better overall accuracy performance than other input bit from a_0 to a_{15} . Using the same method, the second extra signature is chosen after the generation of the signatures of CA and a_6 .

Table 22 lists the number of extra signatures and the corresponding signatures chosen from 16 input bits (a_0 to a_{15}). Note that for 16-bit fixed-width squarer design, the number of extra signatures considered is no more than seven because when the number of extra signatures reaches eight or goes beyond eight, energy consumption and area increase very rapidly. At the same time, the obtained improvement on E_{max} is limited such that EDE_{max} becomes much bigger.

Second, to further decrease energy consumption and area, as illustrated in Sub-section 2.4, don't cares are introduced to some of groups. Considering about logic complexity, if the compensations for all the groups formed by signatures of CA and extra signatures are implemented precisely, an ECU with a complex logic will be generated through logic synthesis, though the error may be minimized. In order to simplify ECU design and tradeoff between cost and error, we set compensation values of

some groups which don't contribute much of the overall error to be don't cares so that the overall error won't be increased dramatically.

For example, to minimize overall E_{max} , we may rank the groups based on their greatest E_{max} , which is defined as the biggest E_{max} that the groups can reach when $\bar{\theta}$ is any value in its range. Since $\bar{\theta}$ has three bits in this case, it ranges from 0 to 7 in decimal number. After the groups are ranked by greatest E_{max} , those which have smaller greatest E_{max} are given a higher priority to be set as don't cares.

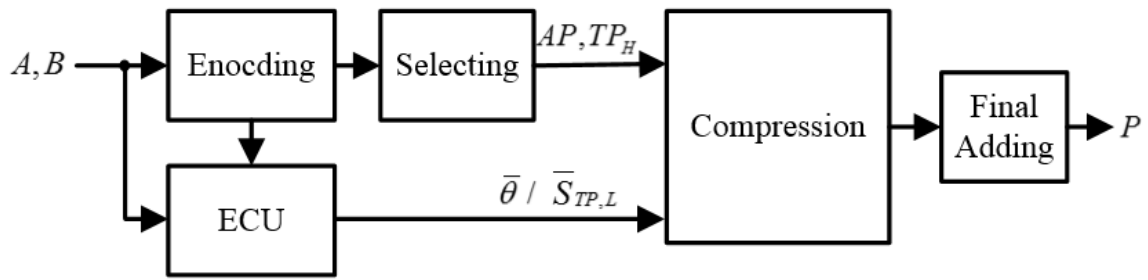
In practice, the more don't cares we set, the less energy consumption and area the design can achieve with the use of a logic synthesis tool such as Synopsis Design Compiler [22], and the bigger E_{max} it is likely to have. Therefore, the number of don't care set for groups should be chosen by jointly considering based on the specifications of energy, delay, area and E_{max} (or other targeted error metric).

5. COMPRESSORS FOR MULTIPLIER AND SQUARER DESIGN

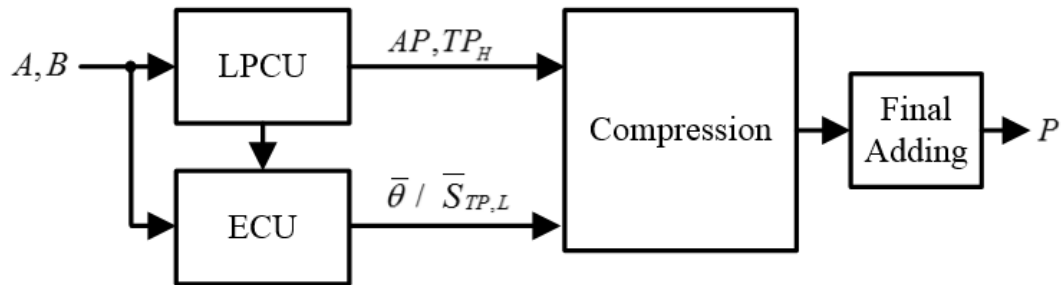
Fig. 12 shows the complete design of the proposed multiplier (a), the details of which is presented in Section 3, and the proposed squarer (b), the details of which is presented in Section 4. For proposed multiplier design, the encoding block applies the Radix-4 Booth Algorithm to encode the multiplier B, allowing the selection block to generate only half number of partial products needed for array multipliers with each product being one of the following: 0, A, 2A, -A, -2A (shown in Fig. 8). For the proposed squarer design, the similar partial product table shown in Fig. 11 is generated.

After the dots which stand for partial products and contain AP , TP_H and $\bar{\theta}$ (for fixed-width designs) or $\bar{S}_{TP,L}$ (for full-width designs), shown in Fig. 8 for multipliers and Fig. 11 for squarers, are generated, they are compressed to only two partial products by compressors in the compression block. Finally, the two partial products are fed into the final adding block and the final result is generated using a Carry propagation adder (CPA).

The purpose of using compressors in the compression block is that multiple compressors can run in parallel, thus speeding up the compression process. In this section, we discuss three types of comparatively low-cost compressors (2:2 Compressors [20], 3:2 Compressors [20] and 4:2 Compressors [21]) that are used in the proposed multiplier and squarer design because they have comparatively less energy and delay overhead. We also discuss the processing steps involved in compression in which multiple compressors run in parallel.



(a)



(b)

Figure 12. Complete designs blocks: (a) the proposed multipliers, (b) the proposed squarers.

5.1 2:2 Compressors

2:2 Compressors have the same function as half adders. 2:2 Compressors help to compress two 1-bit inputs into one 2-bit output. The logic function of 2:2 compressors is presented below

$$\begin{array}{r}
 in1 \\
 + \quad in2 \\
 \hline
 out2 \quad out1 \\
 out1 = in1 \oplus in2 \\
 out2 = in1 \wedge in2
 \end{array}$$

where $in1$, $in2$ are 1-bit inputs, $\{out2, out1\}$ is the 2-bit output and \oplus denotes ‘xor’ operation, the block of 2:2 compressors is shown in Fig. 13.

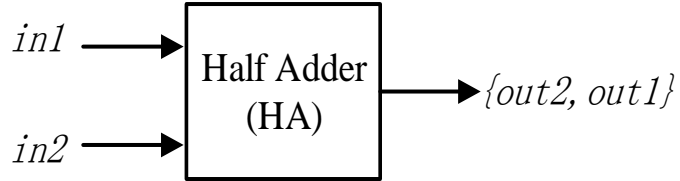


Figure 13. Block diagram of a 2:2 compressor.

5.2 3:2 Compressors

3:2 Compressors [20] have the same function as full adders. 3:2 Compressors help to compress three 1-bit inputs into one 2-bit output. The logic function of 3:2 compressors is presented below

$$\begin{array}{r}
 in1 \\
 in2 \\
 + \quad in3 \\
 \hline
 out2 \quad out1
 \end{array}$$

$$out1 = in1 \oplus in2 \oplus in3$$

$$out2 = in1 \wedge in2 \wedge in3$$

where $in1$, $in2$ and $in3$ are 1-bit inputs, $\{out2, out1\}$ is the 2-bit output, the block of 3:2 compressors is shown in Fig. 14.

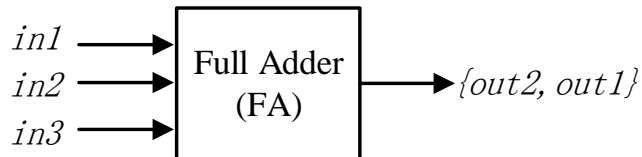


Figure 14. Blocks of a 3:2 compressor.

5.3 4:2 (5:3) Compressors

The logic function of 4:2 (5:3) compressors [21] is presented below. 4:2 compressors have better speed performance than 2:2 and 3:2 compressors but with higher energy consumption and area overhead.

in1

in2

in3

in4

+ *in5*

out2 out1

out3

$$out1 = in1 \oplus in2 \oplus in3 \oplus in4 \oplus in5$$

$$out2 = (in4 \wedge in5) \vee (in1 \oplus in2 \oplus in3) \vee ((in1 \oplus in2 \oplus in3) \wedge in5)$$

$$out3 = (in1 \wedge in2) \vee (in2 \wedge in3) \vee (in1 \wedge in3)$$

where *in1*, *in2*, *in3*, *in4* and *in5* are 1-bit inputs, {*out2+out3*, *out1*} is the output and \vee denotes 'or' operation.

5.4 Using Compressors to Compress Array-Based Partial Product Table

2:2, 3:2 [20] and 4:2 [21] compressors are applied to the compression block shown in Fig. 13 to compress array-based partial product table such as those shown in Fig. 8 and Fig. 11.

As is presented in early this section, the reason why compressors are used in the compression block is that multiple compressors can run in parallel so that the

compression process can be sped up significantly. Fig. 15 gives an example of using 2:2 and 3:2 compressors to compress an array-based partial product table (similar with the partial product table in Fig. 8 for the multiplier design and Fig. 11 for the squarer design), where c1, c2, c3, c4 and c5 are compressors. Again, the purpose of compression process is to compress the number of partial products to only two. Specifically, from right to left, c1 is a 2:2 compressor, c2 is a 3:2 compressor, c3 is a 3:2 compressor, c4 is a 3:2 compressor and c5 is a 2:2 compressor. The dots above the solid line are inputs of the compression block and the dots below the solid line are outputs of the compression block in this case.

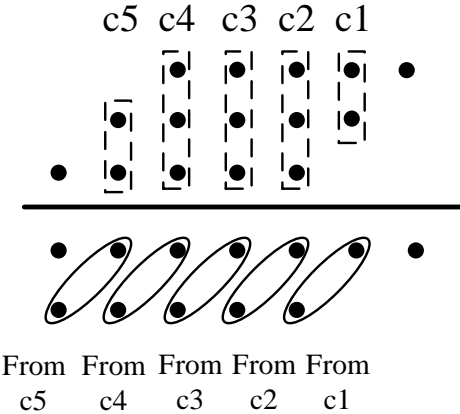


Figure 15. Using 2:2 and 3:2 compressors to compress an array-based partial product table.

As is shown in this example, by using 2:2 and 3:2 compressors, the three partial products (represented by three rows above the solid line) are compressed into a two partial products (represented by two rows below the solid line) and compressors of c1, c2, c3, c4, c5 run in parallel. If no compressors are used and the compression process is made to run in serial, signals on the third column from right can't be compressed until

the carry-out of the second column from the right is calculated and added to the third column from right, the compression of the fourth column from the right is delayed by the third column from the right, and the compression of the fifth column from the right has to wait for the carry-out generated by the compression of fourth column from the right.

6. EXPERIMENTAL RESULTS

The proposed 16-bit fixed-width Booth multiplier and squarer are designed in Verilog HDL, synthesized using Synopsis Design Compiler [17] with a commercial 90 nm CMOS technology and standard cell library. From Synopsis Design Compiler synthesis (Design Vision) reports, we get the pre-layout delay, dynamic power, leakage power and area.

We also implement four additional fixed-width Booth multipliers: DTM (Direct Truncated Booth Multiplier) [5], PEBM (with probabilistic estimation bias compensation) [8], ZSM (uses sum of \bar{z}_i as signatures) [7] and PTM (Post Truncated Booth Multiplier — most accurate/expensive fixed-width multiplier) [3] for comparison purposes.

Four additional squarers are implemented: DTS (Direct Truncated Squarer), CCS (with a constant compensation) [9], VCS (the signals on the $n - 2^{th}$ column as the compensation) [10] and PTS (Post Truncated Squarer — most accurate/expensive fixed-width squarer).

For all Booth multiplier and squarer designs implemented in this research, partial products are generated and then compressed to two partial products using 2:2, 3:2 [20] and 4:2 [21] compressors. As demonstrated in Section 5, 2:2, 3:2 and 4:2 compressors provide an efficient method for compressing the number of partial products to two because they enable the compression process to run in parallel.

Finally, the two compressed partial products are added up by a carry propagation adder (CPA) to produce final results.

6.1 Comparison of Different Multipliers

In Table 6, five fixed-width multipliers are compared in terms of area, delay, power (sum of dynamic power and leakage power), energy and E_{ms} .

The energy consumption and area of the proposed 16-bit fixed-width multiplier are slightly larger than PEBM and ZSM, but are much smaller than PTM, with a 44.85% and 28.33% reduction respectively. On the other hand, the proposed design has a significantly reduced E_{ms} compared with DTM, PEBM and ZSM. This indicates that our design delivers a much improved accuracy with a very small amount of additional overhead compared with PEBM and ZSM. A detailed accuracy comparison will be given in the next section.

Multiplier	Area (μm^2)	Delay (ns)	Power (mW)	Energy (pJ)	E_{ms}
DTM	2,645	2.61	0.86	2.24	9.85
PTM	5,239	3.72	1.75	6.51	0.08
PEBM	2,937	2.79	0.98	2.73	0.35
ZSM	3,256	2.99	1.11	3.32	0.20
Proposed	3,755	2.99	1.20	3.59	0.15

Table 6. Implementation results of different 16x16 bits fixed-width Booth multipliers.

In order to give an overall comparison between the proposed fixed-width 16x16 multiplier design and other approximate fixed-width Booth multipliers, an energy-delay-mean square error product $Energy \cdot Delay \cdot E_{ms}$ (EDE_{ms}) is introduced to evaluate different approximate designs.

Table 7 lists the EDE_{ms} of DTM, PTM, PEBM, ZSM and the proposed 16-bit fixed width Booth multiplier. Fig. 16 lists the EDE_{ms} reduction of the proposed 16x16 bits fixed-width multipliers over DTM, PTM, PEBM and ZSM.

Multiplier	EDE_{ms} ($pJ \cdot ns$)
DTM	57.59
PTM	1.94
PEBM	2.67
ZSM	1.99
Proposed	1.61

Table 7. EDE_{ms} of 16x16 fixed-width multipliers.

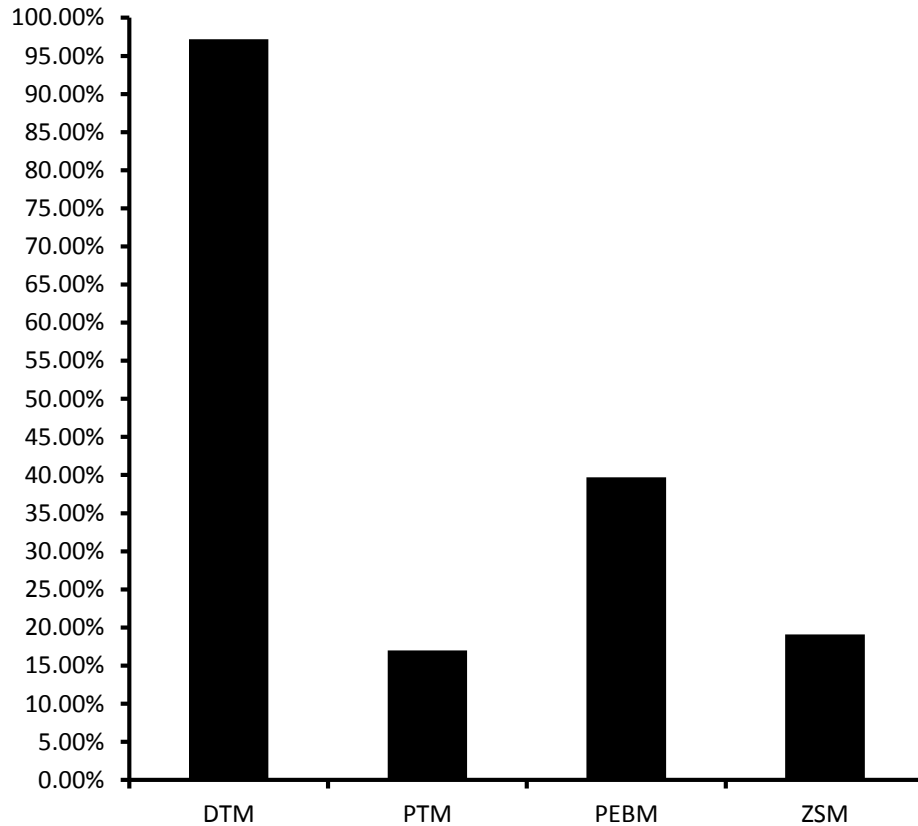


Figure 16. EDE_{ms} reduction of the proposed 16x16 bits fixed-width multipliers over DTM, PTM, PEBM and ZSM.

The proposed multiplier has a significantly reduced EDE_{ms} compared with DTM, PTM, PEBM and ZSM, with 97.20% reduction over DTM, 17.01% reduction over PTM, 39.70% reduction over PEBM and 19.10% reduction over ZSM, respectively. Therefore, the proposed 16-bit multiplier has the best overall performance among the five existing approximate Booth multiplier designs.

6.2 Accuracy Analysis for the Approximate Multipliers

In this section, we provide a more detailed accuracy comparison among different approximate multipliers. Error reduction or accuracy improvement of the proposed design over the existing designs is defined as $\frac{|E_{existing} - E_{proposed}|}{E_{existing}} \times 100\%$, where $E_{existing}$ is one of error metrics (E_{ave} , E_{max} and E_{ms}) of the compared existing design and $E_{proposed}$ is defined as one of error metrics (E_{ave} , E_{max} and E_{ms}) of the proposed design.

6.2.1 Fixed-Width Booth Multipliers

We evaluate the accuracies of the five different designs in terms of E_{ave} , E_{max} and E_{ms} (Section 2.1) for $n = 8$ (bits) in Table 8.

Multiplier	E_{ave}	E_{max}	E_{ms}
DTM	1.50	4.00	2.69
PTM	0.25	0.50	0.08
PEBM	0.35	1.50	0.18
ZSM	0.30	1.17	0.14
Proposed	0.29	1.00	0.13

Table 8. Error metrics of 8x8 fixed-width Booth multipliers.

Fig. 17 shows the error reductions of the proposed fixed-width Booth multiplier over DTM, PEBM and ZSM for $n = 8$ (bits). The achieved reductions are 3.33%, 14.53% and 7.14% in terms of E_{ave} , E_{max} and E_{ms} , respectively, when compared with ZSM.

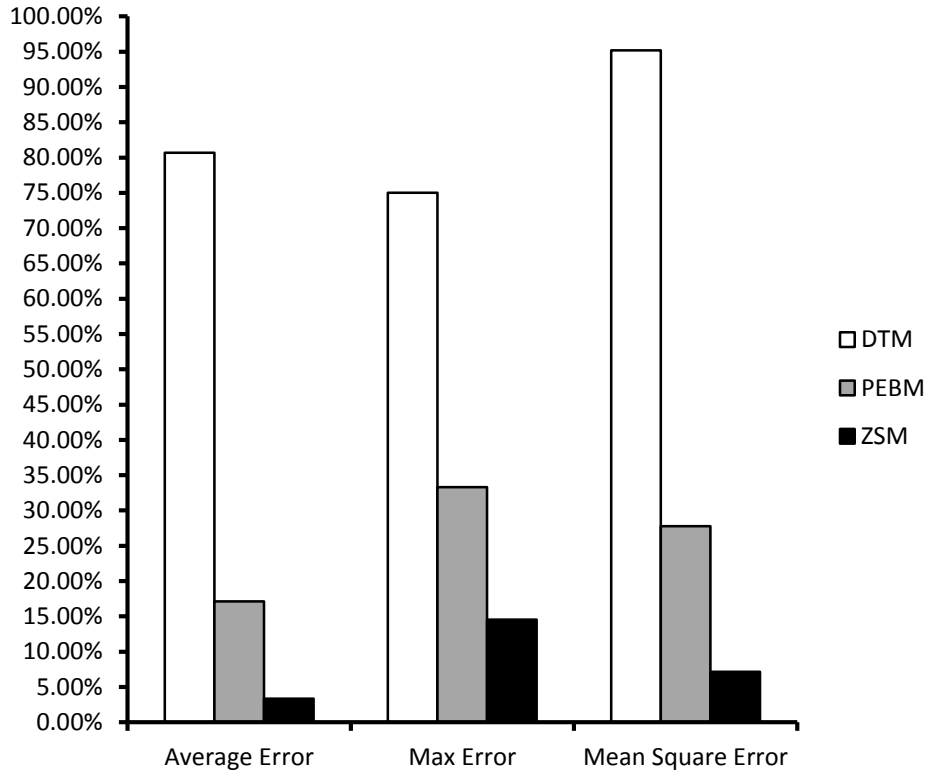


Figure 17. Error reduction of the proposed 8x8 fixed-width Booth multiplier over DTM, PEBM, ZSM.

Multiplier	E_{ave}	E_{max}	E_{ms}
DTM	2.25	6.00	5.71
PTM	0.25	0.50	0.08
PEBM	0.40	2.00	0.25
ZSM	0.33	1.67	0.17
Proposed	0.30	1.46	0.14

Table 9. Error metrics of 12x12 fixed-width Booth multipliers.

Then, we evaluate the accuracies of the five different designs in terms of E_{ave} , E_{max} and E_{ms} (Section 2.1) for $n = 12$ (bits) in Table 9.

Fig. 18 shows the significant error reductions of the proposed fixed-width multipliers over DTM, PEBM and ZSM for $n = 12$ (bits). The achieved reductions are 9.09%, 12.57% and 17.65% in terms of E_{ave} , E_{max} and E_{ms} , respectively, when compared with ZSM.

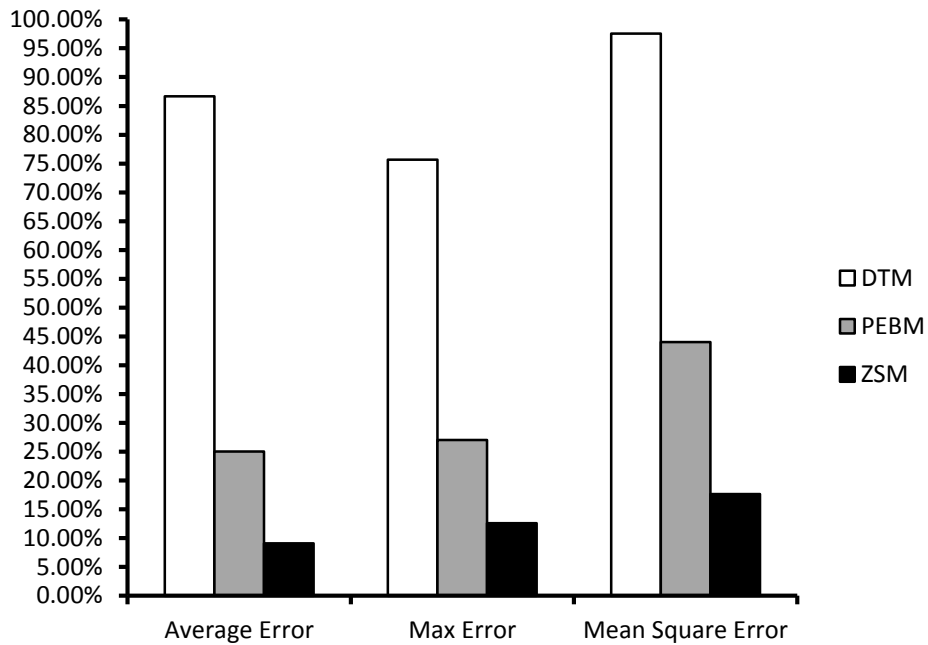


Figure 18. Error reduction of the proposed 12x12 fixed-width Booth multiplier over DTM, PEBM, ZSM.

Multiplier	E_{ave}	E_{max}	E_{ms}
DTM	3.00	8.00	9.85
PTM	0.25	0.50	0.08
PEBM	0.48	2.50	0.35
ZSM	0.36	2.17	0.20
Proposed	0.32	1.56	0.15

Table 10. Error metrics of 16x16 fixed-width Booth multipliers.

Besides, we evaluate the accuracies of the five different designs in terms of E_{ave} , E_{max} and E_{ms} (Section 2.1) for $n = 16$ (bits) in Table 10.

Fig. 19 shows the significant error reductions of the proposed fixed-width multipliers over DTM, PEBM and ZSM for $n = 16$ (bits). The achieved reductions are 11.11%, 28.11% and 25.00% in terms of E_{ave} , E_{max} and E_{ms} , respectively, when compared with ZSM.

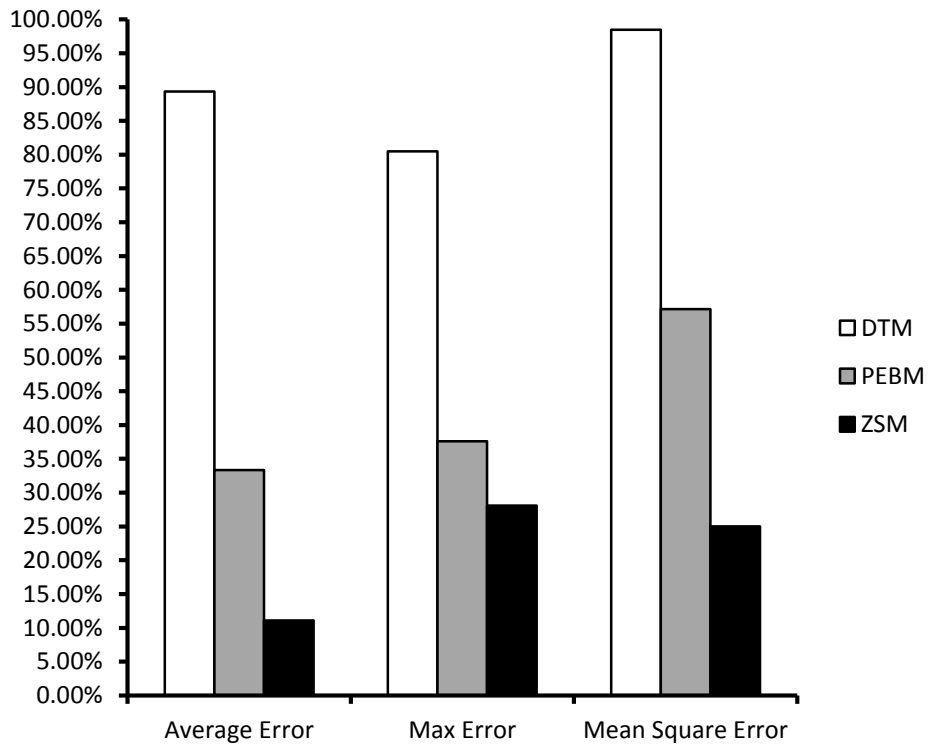


Figure 19. Error reduction of the proposed 16x16 fixed-width Booth multiplier over DTM, PEBM, ZSM.

Lastly, to evaluate the performance of our approach for much wider multipliers, we evaluate the accuracies of the five different designs in terms of E_{ave} , E_{max} and E_{ms} (Section 2.1) for $n = 32$ (bits). Since the number of input cases is very large, exact error

analysis becomes extremely time-consuming. To alleviate the computational challenge while getting decent error estimates, we evaluate each error metric by averaging over a large number of input combinations as follows. For example, for E_{ave} evaluation, we first randomly generate one data set of 400 million input combinations and calculate E_{ave} for this set. To give a more decent and accurate error estimates, we randomly generate 10 such data sets in total, with 400 million input combinations for each set, and calculate the *average* E_{ave} of the ten sets and get the final E_{ave} result.

Fig. 20 shows the significant error reductions of the proposed fixed-width multipliers over DTM, PEBM and ZSM for $n = 32$ (bits). The achieved reductions are 19.89%, 33.79% and 36.90% in terms of E_{ave} , E_{max} and E_{ms} , respectively, when compared with ZSM.

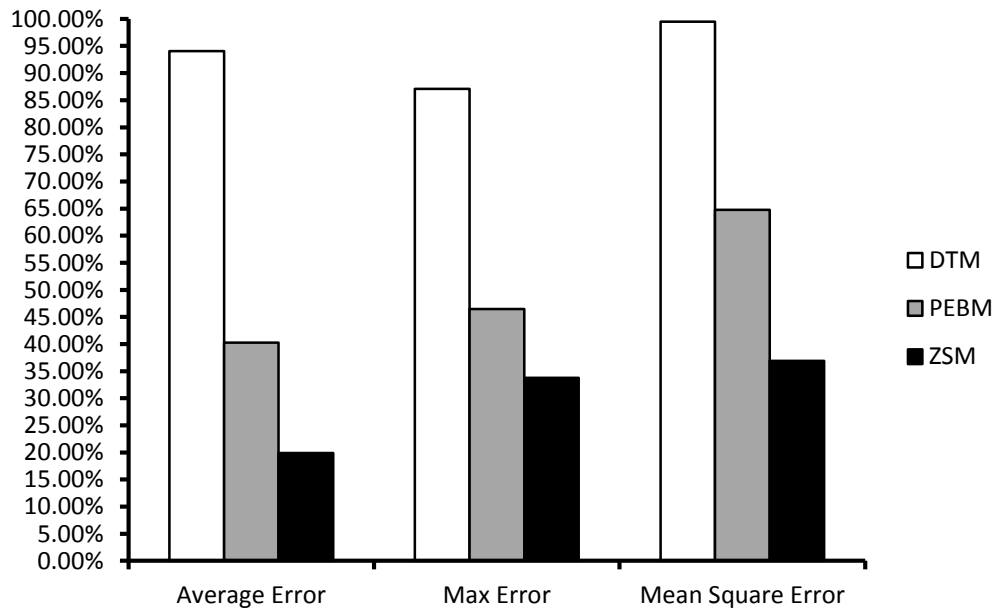


Figure 20. Error reduction of the proposed 32x32 fixed-width Booth multiplier over DTM, PEBM, ZSM.

6.2.2 Full-Width Booth Multipliers

We further evaluate the accuracies of the five different designs operated in full-width mode in terms of E_{ave} , E_{max} and E_{ms} (Section 2.1) for $n = 8$ (bits) in Table 11.

Multiplier	E_{ave}	E_{max}	E_{ms}
PEBM	0.28	1.25	0.12
ZSM	0.21	0.95	0.07
Proposed	0.17	0.59	0.04

Table 11. Error metrics of 8x8 full-width Booth multipliers.

Fig. 21 shows the significant error reductions of the proposed full-width multipliers over PEBM and ZSM for $n = 8$. The achieved reductions are 19.05%, 37.89% and 42.86% in terms of E_{ave} , E_{max} and E_{ms} , respectively, when compared with ZSM. Additionally, the proposed full-width outperforms the most accurate fixed-width PTM with an error reduction of 32.00% and 50.00% for E_{ave} and E_{ms} , respectively, when $n = 8$ (bits).

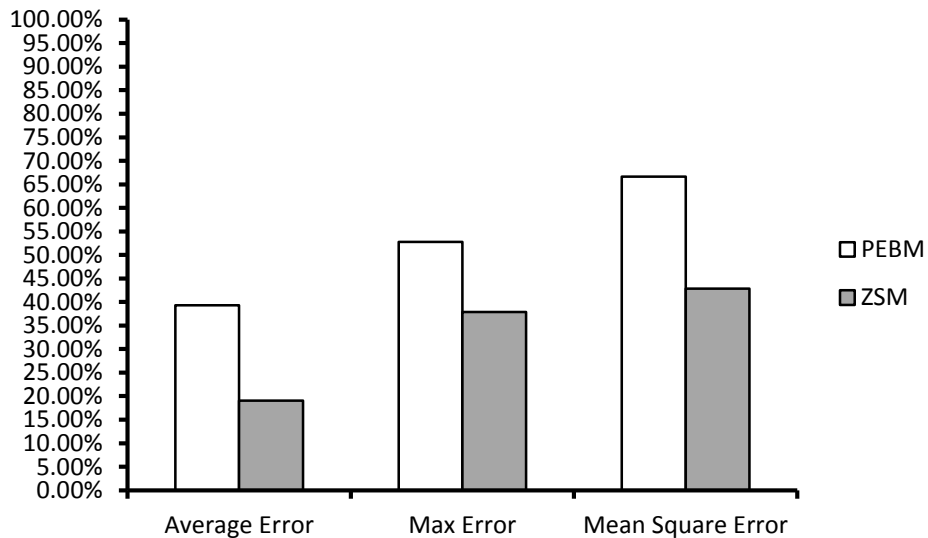


Figure 21. Error reduction of the proposed 8x8 full-width Booth multiplier over PEBM, ZSM.

Then, we evaluate the accuracies of the five different designs operated in full-width mode in terms of E_{ave} , E_{max} and E_{ms} (Section 2.1) for $n = 12$ (bits) in Table 12.

Multiplier	E_{ave}	E_{max}	E_{ms}
PEBM	0.33	1.88	0.17
ZSM	0.25	1.48	0.10
Proposed	0.22	1.10	0.07

Table 12. Error metrics of 12x12 full-width Booth multipliers.

Fig. 22 shows the significant error reductions of the proposed full-width multipliers over PEBM and ZSM for $n = 12$. The achieved reductions are 12.00%, 25.68% and 30.00% in terms of E_{ave} , E_{max} and E_{ms} , respectively, when compared with ZSM. Additionally, the proposed full-width outperforms the most accurate fixed-width PTM with an error reduction of 12.00% and 12.50% for E_{ave} and E_{ms} , respectively, when $n = 12$ (bits).

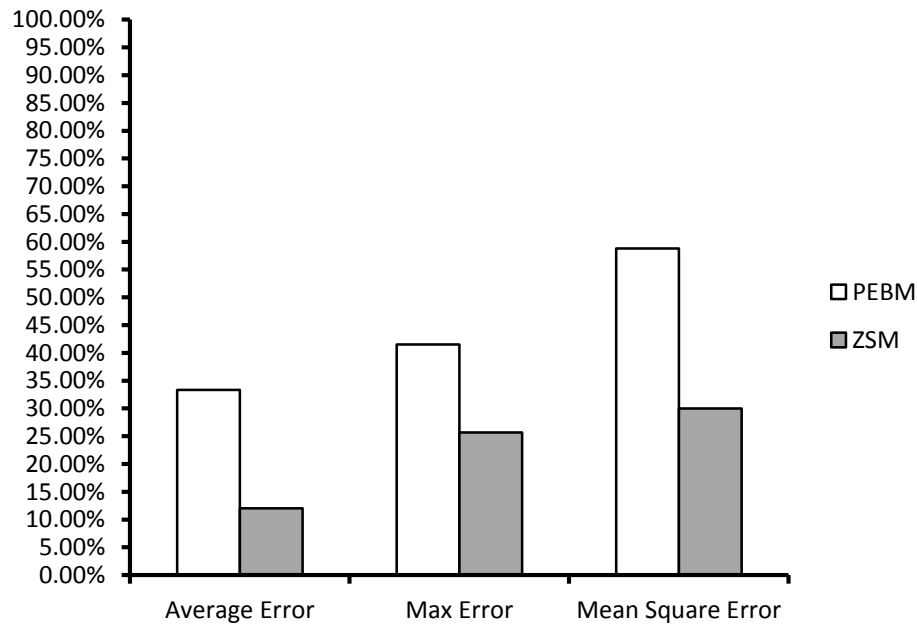


Figure 22. Error reduction of the proposed 12x12 full-width Booth multiplier over PEBM, ZSM.

We evaluate the accuracies of the five different designs operated in full-width mode in terms of E_{ave} , E_{max} and E_{ms} (Section 2.1) for $n = 16$ (bits) in Table 13.

Multiplier	E_{ave}	E_{max}	E_{ms}
PEBM	0.38	2.50	0.22
ZSM	0.29	2.00	0.13
Proposed	0.22	1.25	0.07

Table 13. Error metrics of 16x16 full-width Booth multipliers.

Fig. 23 shows the significant error reductions of the proposed full-width multipliers over PEBM and ZSM for $n = 16$ (bits). The achieved reductions are 24.14%, 37.50% and 46.15% in terms of E_{ave} , E_{max} and E_{ms} , respectively, when compared with ZSM. Additionally, the proposed full-width outperforms the most accurate fixed-width PTM with an error reduction of 12.00% and 12.50% for E_{ave} and E_{ms} , respectively, when $n = 16$ (bits).

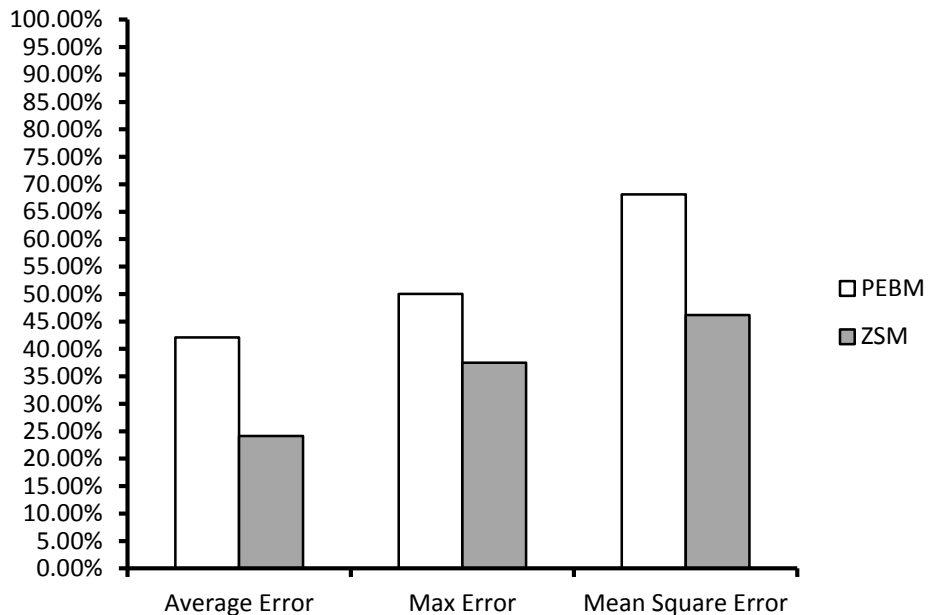


Figure 23. Error reduction of the proposed 16x16 full-width Booth multiplier over PEBM, ZSM.

Lastly, to evaluate the performance of our approach for much wider multipliers, we evaluate the accuracies of the five different designs in terms of E_{ave} , E_{max} and E_{ms} (Section 2.1) for $n = 32$ (bits). Similar to the proposed 32x32 fixed-width multiplier, since the number of input cases is very large, exact error analysis becomes extremely time-consuming. To alleviate the computational challenge while getting decent error estimates, we evaluate each error metric by averaging over a large number of input combinations as follows. For example, for E_{ave} evaluation, we first randomly generate one data set of 400 million input combinations and calculate E_{ave} for this set. To give a more decent and accurate error estimates, we randomly generate 10 such data sets in total, with 400 million input combinations for each set, and calculate the *average* E_{ave} of the ten sets and get the final E_{ave} result.

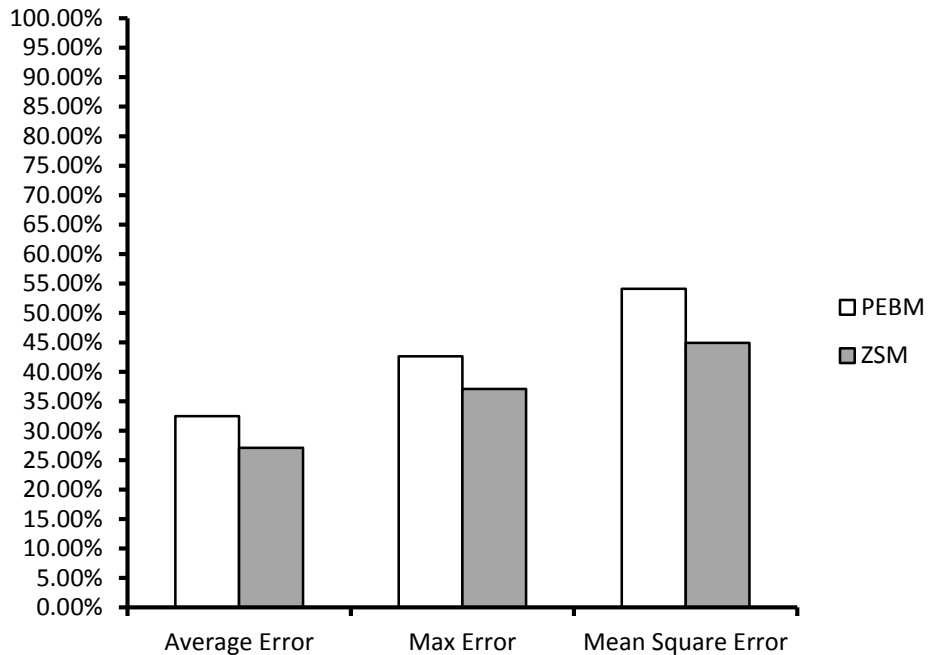


Figure 24. Error reduction of the proposed 32x32 full-width Booth multiplier over PEBM, ZSM.

Fig. 24 shows the significant error reductions of the proposed full-width multipliers over DTM, PEBM and ZSM for $n = 32$, The achieved reductions are 27.09%, 37.09% and 44.93% in terms of E_{ave} , E_{max} and E_{ms} , respectively, when compared with ZSM.

6.3 Comparison of Different Squarers

In Table 14, five fixed-width squarers are compared in terms of area, delay, power (sum of dynamic power and leakage power), energy and E_{ms} .

The energy consumption and area of the proposed multiplier are slightly larger than CCS and VCS, but are much smaller than PTS, with a 42.43% and 30.70% reduction respectively. On the other hand, the proposed design has a significantly reduced E_{ms} compared with DTS, CCS and VCS. This indicates that our design delivers a much improved accuracy with a very small amount of additional overhead. A much detailed accuracy comparison will be given in the next section.

Multiplier	Area (μm^2)	Delay (ns)	Power (mW)	Energy (pJ)	E_{ms}
DTS	1,566	2.21	0.36	0.80	4.34
PTS	3,016	2.93	0.70	2.05	0.08
CCS	1,891	2.22	0.44	0.98	0.28
VCS	1,997	2.34	0.46	1.08	0.16
Proposed	2,090	2.45	0.48	1.18	0.11

Table 14. Implementation results of different 16x16 bits fixed-width squarers.

In order to give an overall comparison between the proposed fixed-width 16x16 bits squarer design and other approximate fixed-width squarers, an energy-delay-mean square error product $Energy \cdot Delay \cdot E_{ms}$ (EDE_{ms}) is utilized to evaluate different approximate designs.

Table 15 lists the value of EDE_{ms} of DTS, PTS, CCS and VCS and the proposed 16-bit fixed-width squarer.

Multiplier	EDE_{ms} ($pJ \cdot ns$)
DTS	7.67
PTS	0.48
CCS	0.61
VCS	0.40
Proposed	0.32

Table 15. EDE_{ms} of 16x16 bits fixed-width squarers.

Fig. 25 lists the EDE_{ms} reduction of the proposed 16x16 bits fixed-width squarers over DTS, PTS, CCS and VCS. The proposed squarer has a significantly reduced EDE_{ms} compared with DTS, PTS, CCS and VCS, with 95.83% reduction over DTS, 33.33% reduction over PTS, 47.54% reduction over CCS and 20.00% reduction over VCS. Therefore, the proposed 16-bit squarer has the best overall performance among the five existing approximate squarer designs.

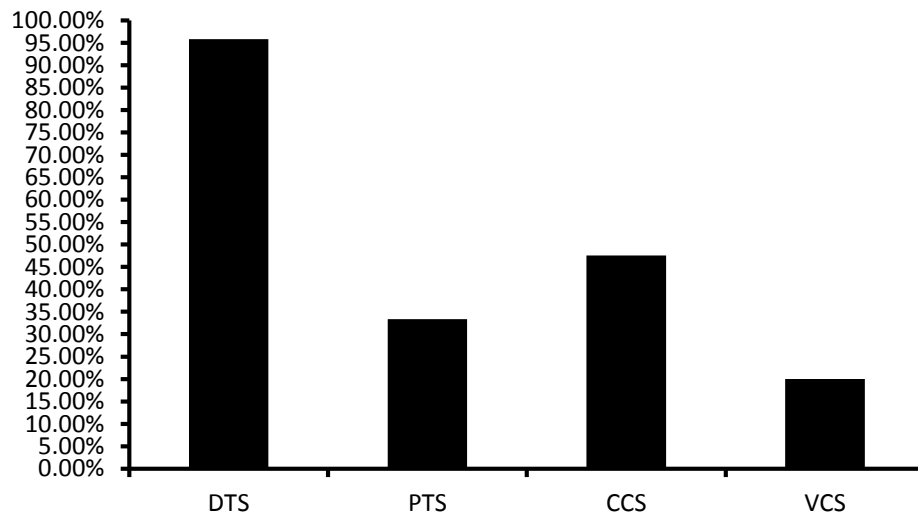


Figure 25. E_{max} reduction of the proposed 16-bit fixed-width squarer over DTS, PTS, CCS and VCS.

6.4 Accuracy Analysis for Squarers

In this section, we provide a more detailed accuracy comparison among different approximate squarers. Similar to multipliers, error reduction or accuracy improvement of the proposed squarer design over the existing designs is defined as $\frac{|E_{existing} - E_{proposed}|}{E_{existing}} \times 100\%$, where $E_{existing}$ is one of error metrics (E_{ave} , E_{max} and E_{ms}) of the compared existing design and $E_{proposed}$ is defined as one of error metrics (E_{ave} , E_{max} and E_{ms}) of the proposed squarer design.

6.4.1 Fixed-Width Squarers

We evaluate the accuracies of the five different designs in terms of E_{ave} , E_{max} and E_{ms} (Section 2.1) for $n = 8$ (bits) in Table 16.

Multiplier	E_{ave}	E_{max}	E_{ms}
DTS	0.83	3.00	1.10
PTS	0.23	0.50	0.08
CCS	0.28	1.10	0.13
VCS	0.29	0.88	0.13
Proposed	0.24	0.75	0.09

Table 16. Error metrics of 8-bit fixed-width squarers.

Fig. 26 shows the significant error reductions of the proposed fixed-width squarers over DTS, CCS and VCS for $n = 8$ (bits). The achieved reductions are 17.24%, 14.77% and 30.77% in terms of E_{ave} , E_{max} and E_{ms} , respectively, when compared with VCS.

Then, we evaluate the accuracies of the five different designs in terms of E_{ave} , E_{max} and E_{ms} (Section 2.1) for $n = 12$ (bits) in Table 17.

Fig. 27 shows the significant error reductions of the proposed fixed-width squarers over DTS, CCS and VCS for $n = 12$ (bits). The achieved reductions are 16.13%, 15.38% and 33.33% in terms of E_{ave} , E_{max} and E_{ms} , respectively, when compared with VCS.

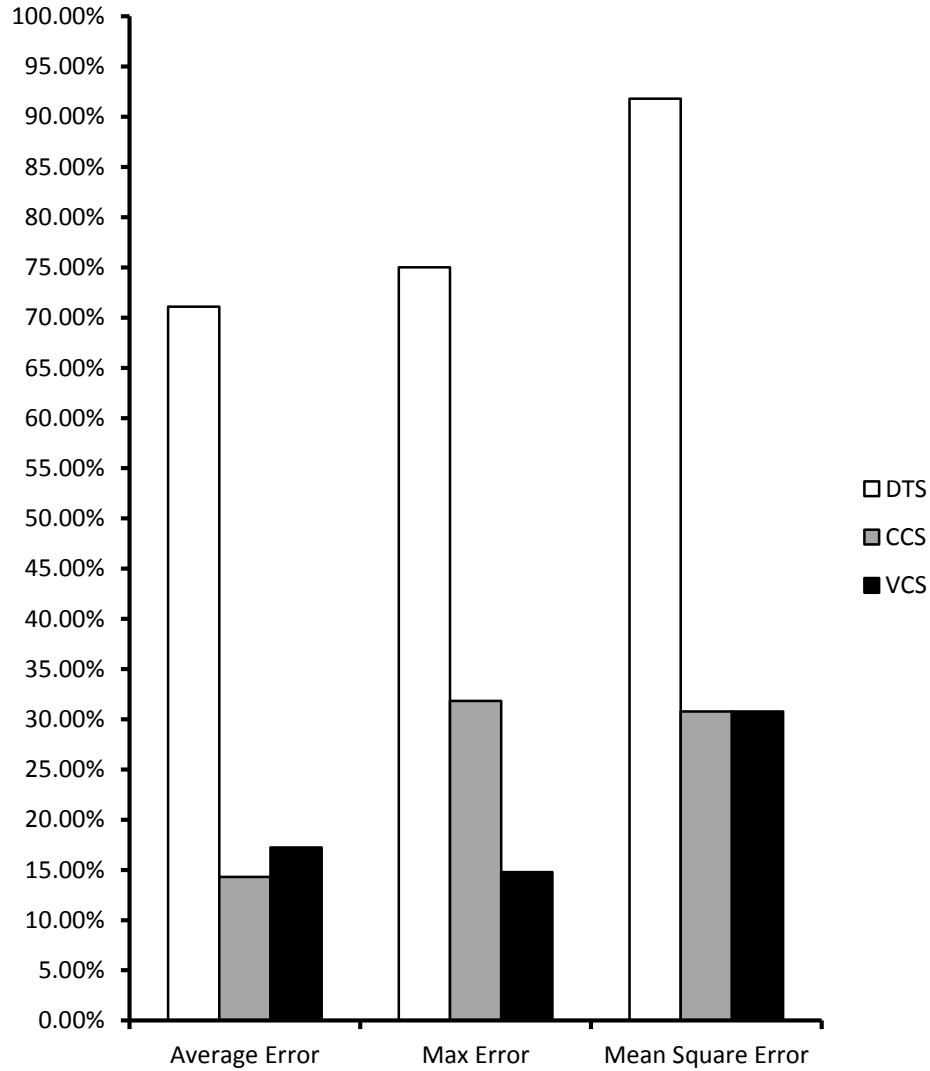


Figure 26. Error reduction of the proposed 8-bit fixed-width squarer over DTS, CCS, VCS.

Multiplier	E_{ave}	E_{max}	E_{ms}
DTS	1.33	5.00	2.46
PTS	0.25	0.50	0.08
CCS	0.40	1.57	0.24
VCS	0.31	1.04	0.15
Proposed	0.26	0.88	0.10

Table 17. Error metrics of 12-bit fixed-width squarers.

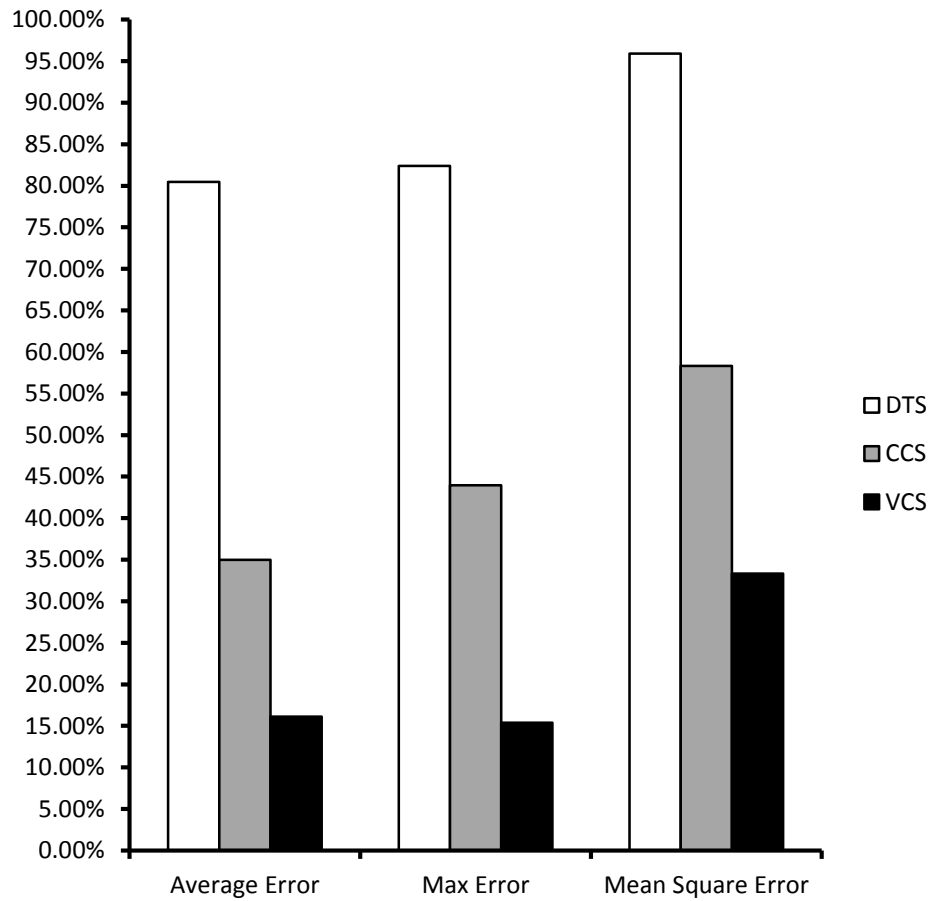


Figure 27. Error reduction of the proposed 12-bit fixed-width squarer over DTS, CCS, VCS.

Lastly, we evaluate the accuracies of the five different designs in terms of E_{ave} , E_{max} and E_{ms} (Section 2.1) for $n = 16$ (bits) in Table 18.

Multiplier	E_{ave}	E_{max}	E_{ms}
DTS	1.83	7.00	4.34
PTS	0.25	0.50	0.08
CCS	0.42	2.56	0.28
VCS	0.33	1.20	0.16
Proposed	0.27	0.94	0.11

Table 18. Error metrics of 16-bit fixed-width squarers.

Fig. 28 shows the significant error reductions of the proposed fixed-width squarers over DTS, CCS and VCS for $n = 16$ (bits). The achieved reductions are 18.18%, 21.67% and 31.25% in terms of E_{ave} , E_{max} and E_{ms} , respectively, when compared with VCS.

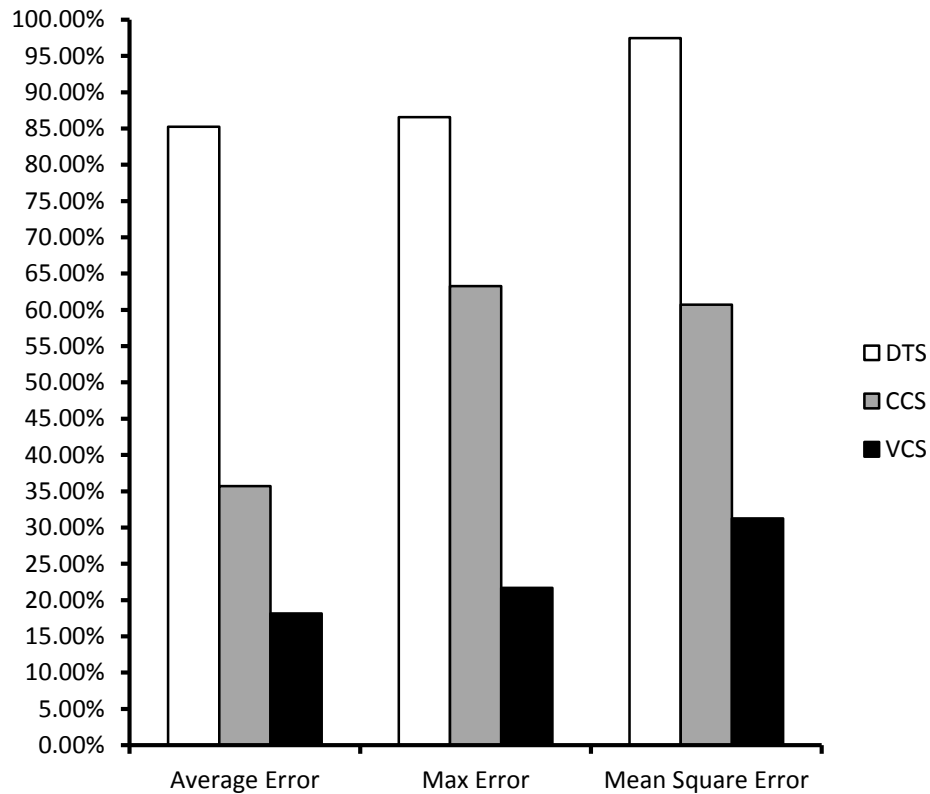


Figure 28. Error reduction of the proposed 16-bit fixed-width squarer over DTS, CCS, VCS.

6.4.2 Full-Width Squarers

We further evaluate the accuracies of the five different designs operated in full-width mode in terms of E_{ave} , E_{max} and E_{ms} (Section 2.1) for $n = 8$ (bits) in Table 19.

Multiplier	E_{ave}	E_{max}	E_{ms}
CCS	0.21	0.76	0.07
VCS	0.15	0.43	0.03
Proposed	0.09	0.35	0.01

Table 19. Error metrics of 8-bit full-width squarers.

Fig. 29 shows the significant error reductions of the proposed full-width squarers over CCS and VCS for $n = 8$ (bits). The achieved reductions are 40.00%, 18.60% and 66.67% in terms of E_{ave} , E_{max} and E_{ms} , respectively, when compared with VCS. Additionally, the proposed full-width design outperforms the most accurate fixed-width PTS with an error reduction of 60.87% and 87.50% for E_{ave} and E_{ms} , respectively, when $n = 8$ (bits).

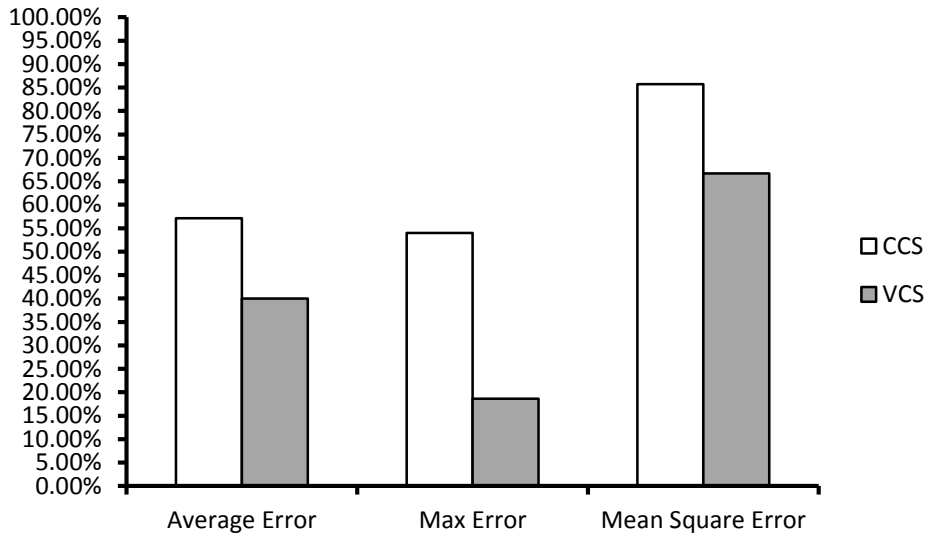


Figure 29. Error reduction of the proposed 8-bit full-width squarer over CCS, VCS.

Then, we evaluate the accuracies of the five different designs operated in full-width mode in terms of E_{ave} , E_{max} and E_{ms} (Section 2.1) for $n = 12$ (bits) in Table 20.

Multiplier	E_{ave}	E_{max}	E_{ms}
CCS	0.30	1.49	0.14
VCS	0.17	0.60	0.05
Proposed	0.12	0.54	0.02

Table 20. Error metrics of 12-bit full-width squarers.

Fig. 30 shows the significant error reductions of the proposed full-width squarers over CCS and VCS for $n = 12$ (bits). The achieved reductions are 29.41%, 10.00% and 60.00% in terms of E_{ave} , E_{max} and E_{ms} , respectively, when compared with VCS. Additionally, the proposed full-width design outperforms the most accurate fixed-width PTS with an error reduction of 52.00% and 75.00% for E_{ave} and E_{ms} , respectively, when $n = 12$ (bits).

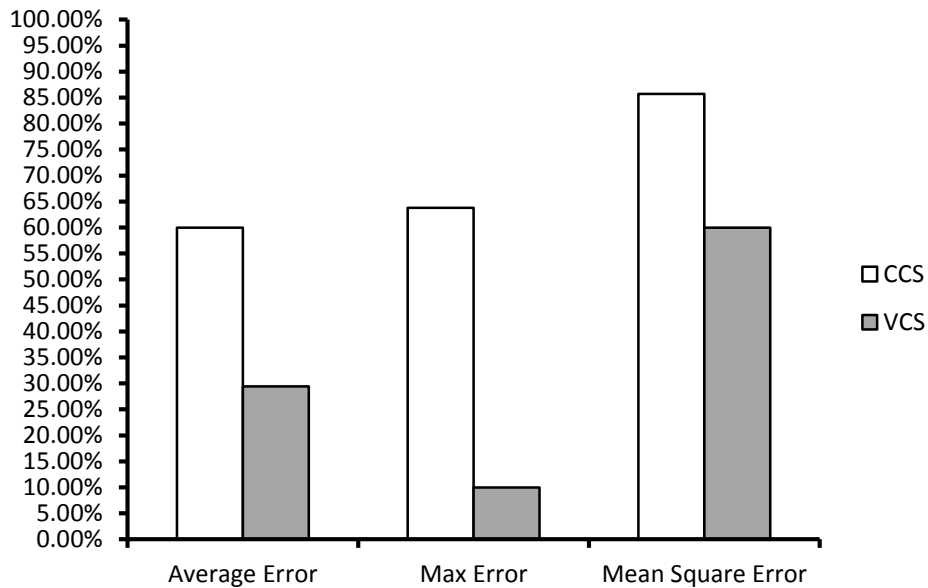


Figure 30. Error reduction of the proposed 12-bit full-width squarer over CCS, VCS.

Finally, we evaluate the accuracies of the five different designs operated in full-width mode in terms of E_{ave} , E_{max} and E_{ms} (Section 2.1) for $n = 16$ (bits) in Table 21.

Multiplier	E_{ave}	E_{max}	E_{ms}
CCS	0.37	2.23	0.21
VCS	0.19	0.77	0.06
Proposed	0.13	0.68	0.03

Table 21. Error metrics of 16-bit full-width squarers.

Fig. 31 shows the significant error reductions of the proposed full-width squarers over CCS and VCS for $n = 16$ (bits). The achieved reductions are 31.58%, 11.69% and 50.00% in terms of E_{ave} , E_{max} and E_{ms} , respectively, when compared with VCS. Additionally, the proposed full-width design outperforms the most accurate fixed-width PTS with an error reduction of 48.00% and 62.50% for E_{ave} and E_{ms} , respectively, when $n = 16$ (bits).

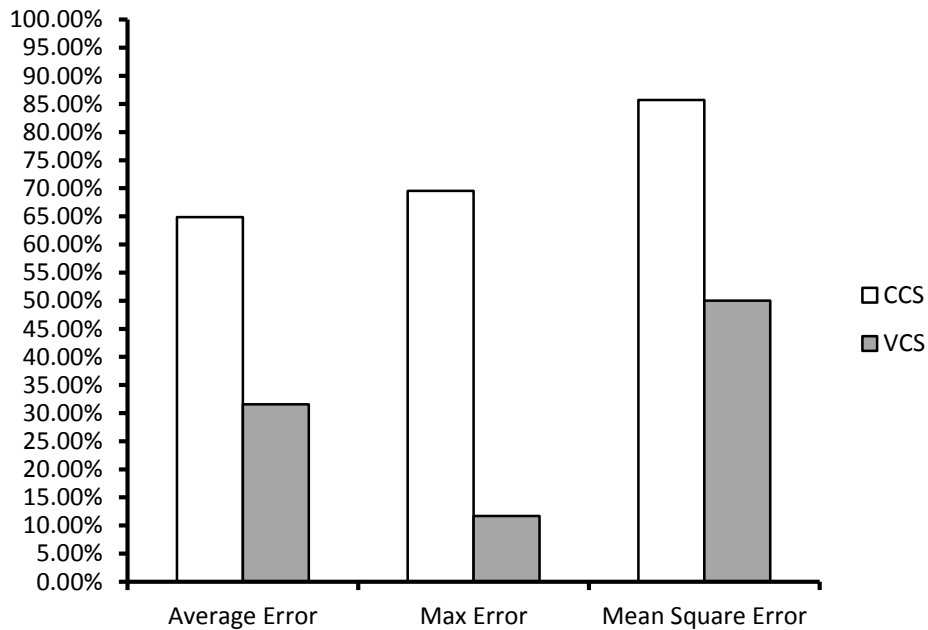


Figure 31. Error reduction of the proposed 16-bit full-width squarer over CCS, VCS.

6.5 Further Reduction of Error and Cost For the 16-bit Fixed-Width Squarer

As illustrated in Section 4.2, we choose extra signatures from input bits (a_0 to a_{15}) and set don't cares to some of the groups to further reduce max error and cost. EDE_{max} , which is the energy-delay-max error product, provides an overall evaluation for 16-bit fixed-width squarer designs.

Table 22 shows the optimal extra signatures from input bits (a_0 to a_{15}), given the number of extra signatures. As described in Section 4.2, for example, to choose one optimal extra signature from the 16 input bits, we try each input bit from a_0 to a_{15} based on the design guidance in Section 2 that efficient signatures should be able to divide input cases into groups largely of equal length (sub-dividing large input groups). The simulation results indicate that selecting a_6 as a signature can divide more original groups formed by the first signature CA and achieve better overall accuracy performance than other input bit from a_0 to a_{15} . Using the same method, the other extra signatures are chosen.

Number of Extra Signatures	Optimal Extra Signature
1	a_6
2	$a_6 a_7$
3	$a_6 a_7 a_{13}$
4	$a_6 a_7 a_{13} a_0$
5	$a_6 a_7 a_{13} a_0 a_4$
6	$a_6 a_7 a_{13} a_0 a_4 a_5$
7	$a_6 a_7 a_{13} a_0 a_4 a_5 a_8$

Table 22. Optimal extra signatures for given number of extra signatures.

The resulting area, delay, power (sum of dynamic power and leakage power), energy consumption and EDE_{max} as a function of the number of extra signatures are

listed in Table 23. Correspond to the last row of the table, when introducing seven extra signatures, to tradeoff between energy consumption and E_{max} , we set 110 groups as don't cares.

Number of Extra Signatures	Area (μm^2)	Delay (ns)	Power (mW)	Energy (pJ)	EDE_{ms}
1	2,090	2.45	0.48	1.18	2.72
2	2,095	2.45	0.48	1.18	2.66
3	2,129	2.45	0.48	1.18	2.46
4	2,137	2.45	0.48	1.18	2.43
5	2,156	2.46	0.48	1.18	2.38
6	2,202	2.48	0.48	1.19	2.36
7	2,295	2.49	0.49	1.22	2.40
7 (introducing don't cares)	2,167	2.46	0.48	1.18	2.29

Table 23. EDE_{max} of 16-bit fixed-width squarers with extra signatures.

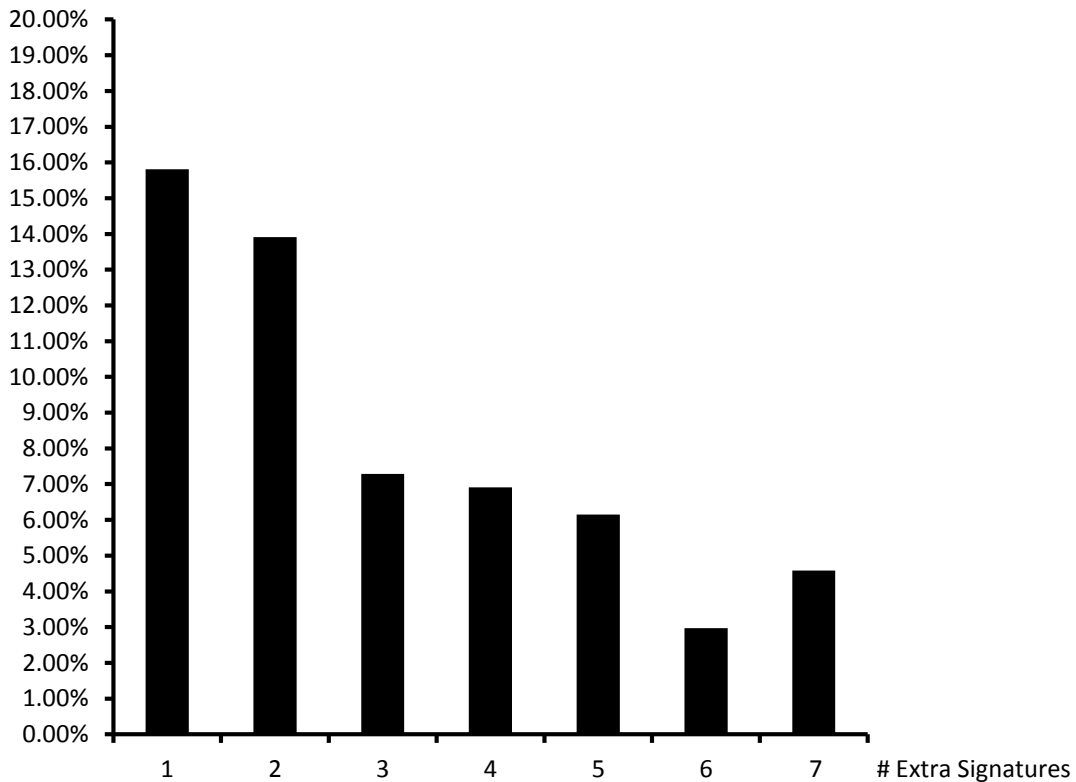


Figure 32. Comparison of EDE_{max} of 16-bit fixed-width squarers with extra input signatures.

Fig. 32 shows the error reduction of optimized 16-bit fixed-width squarer design (seven extra signatures from input bits and setting don't cares for the compensations of 110 groups) to designs with the number of extra signatures ranges from one to seven with no don't cares introduced. As shown in Fig. 32, further optimizing the squarer by introducing seven extra signatures and don't cares decreases EDE_{max} significantly, with 15.81% reduction, when compared with the proposed 16-bit fixed-width squarer design which uses only one extra signature and not introducing any don't cares (the first bar).

7. CONCLUSION

In this research, a general model is presented for array-based approximate arithmetic computing to guide the design of approximate Booth multipliers and squarers. To shed light on the design of ECU, which is the key of AAAC design, we develop four theorems to address two critical design problems of the ECU design, namely, determination of optimal error compensation values and identification of the optimal error compensation scheme. To further reduce energy consumption and area, we introduce don't cares for ECU logic simplification.

Our proposed 16x16 bits fixed-width Booth multiplier consumes 44.85% and 28.33% less energy and area compared with the most accurate fixed-width Booth multiplier. Additionally, a 11.11%, 28.11%, 25.00% and 19.10% reduction is achieved for average error, max error, mean square error and EDE_{ms} , respectively, when compared with the best reported approximate design. Using the same approach, our approximate 16-bit fixed-width squarer reduces average error, max error, mean square error and EDE_{ms} by more than 18.18%, 21.67%, 31.25% and 20.00%, respectively, when compared with existing designs. Error and cost are further reduced by utilizing the method of introducing extra signatures and don't cares, with 15.81% reduction for EDE_{max} . Significant error improvements have also been achieved for proposed multipliers and squarers when operated in full-width mode.

REFERENCES

1. Schulte, Michael J., and Earl E. Swartzlander. "*Truncated multiplication with correction constant [for DSP].*" VLSI Signal Processing, VI, 1993.,[Workshop on]. IEEE, 1993.
2. King, Eric J., and E. E. Swartzlander. "*Data-dependent truncation scheme for parallel multipliers.*" Signals, Systems & Computers, 1997. Conference Record of the Thirty-First Asilomar Conference on. Vol. 2. IEEE, 1997.
3. Jou, Shyh-Jye, Meng-Hung Tsai, and Ya-Lan Tsao. "*Low-error reduced-width Booth multipliers for DSP applications.*" Circuits and Systems I: Fundamental Theory and Applications, IEEE Transactions on 50.11 (2003): 1470-1474.
4. Min-An, S. O. N. G., V. A. N. Lan-Da, and K. U. O. Sy-Yen. "*Adaptive low-error fixed-width Booth multipliers.*" IEICE Transactions on Fundamentals of Electronics, Communications and Computer Sciences 90.6 (2007): 1180-1187.
5. Huang, Hong-An, Yen-Chin Liao, and Hsie-Chia Chang. "*A self-compensation fixed-width booth multiplier and its 128-point FFT applications.*" Circuits and Systems, 2006. ISCAS 2006. Proceedings. 2006 IEEE International Symposium on. IEEE, 2006.
6. Cho, Kyung-Ju, et al. "*Design of low-error fixed-width modified booth multiplier.*" Very Large Scale Integration (VLSI) Systems, IEEE Transactions on 12.5 (2004): 522-531.

7. Wang, Jiun-Ping, Shiann-Rong Kuang, and Shish-Chang Liang. "*High-accuracy fixed-width modified Booth multipliers for lossy applications.*" Very Large Scale Integration (VLSI) Systems, IEEE Transactions on 19.1 (2011): 52-60.
8. Li, Chung-Yi, et al. "*A probabilistic estimation bias circuit for fixed-width Booth multiplier and its DCT applications.*" Circuits and Systems II: Express Briefs, IEEE Transactions on 58.4 (2011): 215-219.
9. Walters III, E. George, Michael J. Schulte, and Mark G. Arnold. "*Truncated squarers with constant and variable correction.*" Optical Science and Technology, the SPIE 49th Annual Meeting. International Society for Optics and Photonics, 2004.
10. Walters III, E. George, and Michael J. Schulte. "*Efficient function approximation using truncated multipliers and squarers.*" Computer Arithmetic, 2005. ARITH-17 2005. 17th IEEE Symposium on. IEEE, 2005.
11. Hoang, Van-Phuc, and Cong-Kha Pham. "*Low-error and efficient fixed-width squarer for digital signal processing applications.*" Communications and Electronics (ICCE), 2012 Fourth International Conference on. IEEE, 2012.
12. Du, Kai, Peter Varman, and Kartik Mohanram. "*High performance reliable variable latency carry select addition.*" Design, Automation & Test in Europe Conference & Exhibition (DATE), 2012. IEEE, 2012.
13. Zhu, Ning, Wang Ling Goh, and Kiat Seng Yeo. "*An enhanced low-power high-speed adder for error-tolerant application.*" Integrated Circuits, ISIC'09. Proceedings of the 2009 12th International Symposium on. IEEE, 2009.

14. Kim, Yongtae, Yong Zhang, and Peng Li. "*An energy efficient approximate adder with carry skip for error resilient neuromorphic VLSI systems.*" Proceedings of the International Conference on Computer-Aided Design. IEEE Press, 2013.
15. Hachtel, Gary D., and Fabio Somenzi. *Logic synthesis and verification algorithms*. Springer, 2006.
16. Bergamaschi, Reinaldo A., et al. "*Efficient use of large don't cares in high-level and logic synthesis.*" Proceedings of the 1995 IEEE/ACM international conference on Computer-aided design. IEEE Computer Society, 1995.
17. Synopsys. Inc., "*Design compiler user guide*" , [http://www. synopsys. com](http://www.synopsys.com), 2010.
18. Weste, Neil, and David Harris. *CMOS VLSI design: a circuits and systems perspective*. Addison-Wesley Publishing Company, 2010.
19. de Angel, Edwin, and E. E. Swartzlander. "*Low power parallel multipliers.*" VLSI Signal Processing, IX, 1996.,[Workshop on]. IEEE, 1996.
20. Wallace, Christopher S. "*A suggestion for a fast multiplier.*" Electronic Computers, IEEE Transactions on 1 (1964): 14-17.
21. Oklobdzija, Vojin G., David Villeger, and Simon S. Liu. "*A method for speed optimized partial product reduction and generation of fast parallel multipliers using an algorithmic approach.*" Computers, IEEE Transactions on 45.3 (1996): 294-306.

22. Batcher, Kenneth E. "*Sorting networks and their applications.*" Proceedings of the April 30--May 2, 1968, spring joint computer conference. ACM, 1968.